Coupled cluster calculations of the frequency-dependent second hyperpolarizabilities of Ne, Ar, N_2, and CH_4

Christof Hättig and Poul Jørgensen
Department of Chemistry, University of Aarhus, DK-8000 Aarhus C, Denmark

(Received 18 February 1998; accepted 12 May 1998)

The recently developed coupled cluster cubic response approach is applied to the calculation of frequency-dependent second hyperpolarizabilities for Ne, Ar, N_2, and CH_4. A basis set investigation is performed for the static hyperpolarizabilities at the Hartree-Fock and the coupled cluster singles and doubles level (CCSD) using series of correlation consistent basis sets. For N_2 and CH_4 we have employed basis set up to, respectively, 326 and 353 basis functions. The role of correlation effects on the dispersion of the hyperpolarizabilities is explored by a comparison of Hartree-Fock, coupled cluster singles (CCS), CC2 and CCSD results for the third harmonic generation. Dispersion curves are calculated at the CCSD level for the dc Kerr effect, degenerate four wave mixing, electric field induced second harmonic generation, and third harmonic generation. For comparison with experiment we have considered zero point vibrational averaging, pure vibrational contributions and corrections for core correlation and connected triples. For all four systems we obtain much better agreement with experiment than in previous *ab initio* calculations. © *1998 American Institute of Physics.* [S0021-9606(98)30431-6]

I. INTRODUCTION

In recent years much effort has focused around experimental and theoretical determination of accurate gas phase hyperpolarizabilities for atoms and small molecules.[1–11] Both, the experimental techniques and the quantum chemical *ab initio* methods have been improved considerably.[6,12–17] However, *ab initio* calculations of frequency-dependent second hyperpolarizabilities with an error tolerance of a couple of percents is still a difficult task that has been accomplished only for two-electron systems.[7,18] Such an accuracy requires a thorough treatment of dynamic electron correlation and large one-particle basis sets. To obtain an accurate description of the dispersion, the frequency-dependence must be accounted for at a correlated level using a wave function model where also the pole structure is described at a correlated level. This is in general only achieved by iterative correlation methods like multiconfiguration self-consistent field (MCSCF), configuration interaction (CI), or coupled cluster (CC) response theory[19–22] and only the last method is expected to be capable of providing accurate results also for larger systems. Noniterative methods based on Møller-Plesset perturbation theory are not able to correlate the pole structure of dynamic properties.[23] For molecules it is also necessary to consider zero point vibrational averaging and pure vibrational contributions to obtain a realistic comparison with experiment.

With the coupled cluster response approach[21,24,25] which recently has been implemented at the CCS, CC2 and CCSD level for dynamic third-[16] and fourth-order properties,[17] a new tool has become available for the calculation of correlated frequency-dependent hyperpolarizabilities. The hierarchy CCS, CC2,[26] CCSD, etc., accounts (beyond the CCS level) efficiently for dynamic electron correlation and gives systematic improvements in the excitation energies, i.e., the poles of dynamic properties, at each level of the hierarchy.[27,28]

In the present study we employ the coupled cluster cubic response approach[17] and series of correlation consistent basis sets[29] to calculate accurate dispersion curves for the second hyperpolarizabilities of Ne, Ar, N_2 and CH_4 for several third-order optical processes, including electric field induced second harmonic generation (ESHG) and third harmonic generation (THG). We have chosen Ne, Ar, N_2 and CH_4, because accurate experimental data that covers a wide range of frequencies is available from the ESHG experiments of Shelton and co-workers.[3,4,6] Thus, for these systems a detailed comparison can be made between the *ab initio* calculated hyperpolarizabilities and accurate experimental dispersion curves. This allows to separate to a certain extent the errors in the frequency-dependence from the errors already present in the static hyperpolarizabilities. With two atoms, a diatom, and a spherical top molecule, the four examples also represent three classes of systems with different convergence of the hyperpolarizabilities with respect to basis set saturation and the importance of vibrational effects.

The paper is organized as follows: In Sec. II we give a brief account of the coupled cluster cubic response approach and discuss the number of response equations that have to be solved for the different third-order optical processes. In Sec. III we report the technical details of the calculations. The results of a basis set investigation at the SCF and the CCSD response level using series of correlation consistent basis sets are discussed in Sec. IV. The importance of orbital relaxation effects and connected triples is discussed in Sec. V. In the same section we compare the performance of the SCF, CCS, CC2 and CCSD response approaches for the dispersion contribution to the third harmonic generation. In Sec. VI we present CCSD dispersion curves for the dc Kerr effect, de-

 © 1998 American Institute of Physics

generate four wave mixing (DFWM), electric field induced second harmonic generation (ESHG), and third harmonic generation (THG) and give a detailed comparison with the available experimental data. In Sec. VII we give some concluding remarks.

II. THE COUPLED CLUSTER CUBIC RESPONSE APPROACH

In the calculation of frequency-dependent hyperpolarizabilities or response functions in general, one considers a system described by $H^{(0)}$ which is subject to one or more oscillating external perturbations:

$$H(t,\boldsymbol{\epsilon}) = H^{(0)} + \sum_j H^{X_j} \boldsymbol{\epsilon}_j(\omega_j) e^{-i\omega_j t}. \tag{1}$$

The coupled cluster response functions are most conveniently derived by combining the time-depending coupled cluster quasienergy[16,17,24]

$$\mathcal{W}(t,\boldsymbol{\epsilon}) = \langle \mathrm{HF} | H(t,\boldsymbol{\epsilon}) \exp(T(t,\boldsymbol{\epsilon})) | \mathrm{HF} \rangle, \tag{2}$$

and the time-dependent cluster amplitude equations,[21]

$$\langle \bar{\mu} | \exp(-T(t,\boldsymbol{\epsilon})) \left(H(t,\boldsymbol{\epsilon}) - i \frac{d}{dt} \right) \exp(T(t,\boldsymbol{\epsilon})) | \mathrm{HF} \rangle = 0, \tag{3}$$

to a quasienergy Lagrangian:[23,24]

$$L = \langle \mathrm{HF} | H \exp(T) | \mathrm{HF} \rangle + \sum_\mu \bar{t}_\mu \langle \bar{\mu} | \exp(-T) \left(H - i \frac{d}{dt} \right) \exp(T) | \mathrm{HF} \rangle. \tag{4}$$

As reference state $|\mathrm{HF}\rangle$ we use the Hartree-Fock wave function for the unperturbed system, i.e., in the coupled cluster response calculations unrelaxed Hartree-Fock orbitals are used and the effects of orbital relaxation are treated only implicitly by the single excitation part of the cluster operator. The amplitudes t_μ of the cluster operator $T = \Sigma_\mu t_\mu \hat{\tau}_\mu$ and the Lagrangian multipliers $\bar{t}_\mu$ can be expanded in the Fourier components and orders of the external field strengths as:

$$t_\mu(t,\boldsymbol{\epsilon}) = \sum_{n=0}^{\infty} \frac{1}{n!} \sum_{j_1} \cdots \sum_{j_n} t_\mu^{X_{j_1} \cdots X_{j_n}}(\omega_{j_1}, \ldots, \omega_{j_n}) \times \prod_{m=1}^{n} \boldsymbol{\epsilon}_{j_m}(\omega_{j_m}) e^{-i\omega_{j_m} t}, \tag{5}$$

$$\bar{t}_\mu(t,\boldsymbol{\epsilon}) = \sum_{n=0}^{\infty} \frac{1}{n!} \sum_{j_1} \cdots \sum_{j_n} \bar{t}_\mu^{X_{j_1} \cdots X_{j_n}}(\omega_{j_1}, \ldots, \omega_{j_n}) \times \prod_{m=1}^{n} \boldsymbol{\epsilon}_{j_m}(\omega_{j_m}) e^{-i\omega_{j_m} t}, \tag{6}$$

where the coefficients $t_\mu^{X_1 \cdots X_n}$ and $\bar{t}_\mu^{X_1 \cdots X_n}$ are defined as derivatives, i.e., they are symmetric with respect to permutation of the operator/frequency pairs (X_i, ω_i). In the presence of a (quasi-) periodic perturbation, as we consider here, the time-evolution of the system is completely determined by the condition that the time-average of the quasienergy Lagrangian is stationary with respect to variations of the cluster amplitudes and the Lagrangian multipliers:[20,24,30]

$$\delta \left\{ \lim_{t_0 \to \infty} \frac{1}{2t_0} \int_{-t_0}^{t_0} L(t,\boldsymbol{\epsilon}) dt \right\} = 0. \tag{7}$$

Inserting the ansatz for the cluster amplitudes (5) and the Lagrangian multipliers (6) into the stationary condition, Eq. (7) becomes a set of response equations for the Fourier components of t_μ and $\bar{t}_\mu$. In zeroth-order one obtains the usual unperturbed coupled cluster equations and the equations for the zeroth-order Lagrangian multipliers:

$$\sum_\mu \bar{t}_\mu^{(0)} A_{\mu\nu} = \langle \mathrm{HF} | \exp(-T^{(0)}) [H^{(0)}, \tau_\nu] \exp(T^{(0)}) | \mathrm{HF} \rangle, \tag{8}$$

where the matrix $\boldsymbol{A}$ is the coupled cluster Jacobian, defined as

$$A_{\mu\nu} = \left(\frac{\partial^2 L}{\partial \bar{t}_\mu \partial t_\nu} \right)_{\boldsymbol{\epsilon}_i = 0}. \tag{9}$$

The formulation of response functions as derivatives of a variational functional allows us to employ the $2n+1$ and $2n+2$ rules[31,32] in the calculation of frequency-dependent response properties. Thus, for the cubic response function we need in addition to the zeroth-order equations also solve the first-order response equations for the cluster amplitudes and the Lagrangian multipliers,

$$(\boldsymbol{A} - \omega \mathbf{1}) t^X(\omega) = -\xi^X, \tag{10}$$

$$\bar{t}^X(\omega)(\boldsymbol{A} + \omega \mathbf{1}) = -(\boldsymbol{\eta}^X + \boldsymbol{F} t^X(\omega)), \tag{11}$$

and the second-order response equations for the cluster amplitudes,

$$(\boldsymbol{A} - (\omega_1 + \omega_2)\mathbf{1}) t^{X_1 X_2}(\omega_1, \omega_2) = -\hat{P}^{X_1 X_2} \left(\tfrac{1}{2} \boldsymbol{B} t^{X_1}(\omega_1) t^{X_2}(\omega_2) + \boldsymbol{A}^{X_1} t^{X_2}(\omega_2) \right), \tag{12}$$

where the vectors ξ^X and η^X and the matrices $\boldsymbol{F}$, $\boldsymbol{B}$, and $\boldsymbol{A}^X$ are defined as derivatives of the quasienergy Lagrangian:

$$\xi_\mu^A = \left(\frac{\partial^2 L}{\partial \boldsymbol{\epsilon}_A(\omega_A) \partial \bar{t}_\mu} \right)_{\boldsymbol{\epsilon}_i = 0}, \tag{13}$$

$$\eta_\mu^A = \left(\frac{\partial^2 L}{\partial \boldsymbol{\epsilon}_A(\omega_A) \partial t_\mu} \right)_{\boldsymbol{\epsilon}_i = 0}, \tag{14}$$

$$F_{\mu\nu} = \left(\frac{\partial^2 L}{\partial t_\mu \partial t_\nu} \right)_{\boldsymbol{\epsilon}_i = 0}, \tag{15}$$

$$B_{\mu\nu\gamma} = \left(\frac{\partial^3 L}{\partial \bar{t}_\mu \partial t_\nu \partial t_\gamma} \right)_{\boldsymbol{\epsilon}_i = 0}, \tag{16}$$

$$A_{\mu\nu}^A = \left(\frac{\partial^3 L}{\partial \boldsymbol{\epsilon}_A(\omega_A) \partial \bar{t}_\mu \partial t_\nu} \right)_{\boldsymbol{\epsilon}_i = 0}. \tag{17}$$

The operator $\hat{P}^{X_1 \cdots X_n}$ symmetrizes with respect to permutations of the operators $X_1, \ldots, X_n$ together with the accompanied frequencies $\omega_1, \ldots, \omega_n$. The response functions are obtained as derivatives of the real part of the time-averaged quasienergy Lagrangian with respect to the field strengths:

$$\langle\langle X_0; X_2, \ldots, X_n \rangle\rangle_{\omega_1, \ldots, \omega_2} = \left(\frac{d^n \{ \frac{1}{2} L(t,\epsilon) + \frac{1}{2} L(t,\epsilon)^* \}}{d\epsilon_0(\omega_0) \cdots d\epsilon_n(\omega_n)} \right)_{\epsilon_i = 0}. \quad (18)$$

The explicit symmetrization with respect to complex conjugation of $L(t,\epsilon)$ is neccessary because the coupled cluster (quasi-) energy is defined by the projection type expression $\langle \mathrm{HF}|H\exp(T)|\mathrm{HF}\rangle$ which in general gives complex results if H is complex.[16,22] Taking the derivative of only the real part of $L(t)$ guarantees the so-called time-reversal symmetry[33] of the response functions:

$$\langle\langle X_0; X_1, \ldots, X_n \rangle\rangle_{-\omega_1, \ldots, -\omega_n} = \langle\langle X_0; X_1, \ldots, X_n \rangle\rangle^*_{\omega_1, \ldots, \omega_n}. \quad (19)$$

In the case of the real hyperpolarizabilities the time-reversal symmetry reduces to symmetry with respect to an overall sign change of the frequency arguments. The cubic response function is obtained as the fourth derivative of the real part of $L(t,\epsilon)$. Keeping only terms in accordance with the $2n+1$ and $2n+2$ rules we obtain:

$$\begin{aligned} \langle\langle A; B, C, D \rangle\rangle_{\omega_B, \omega_C, \omega_D} = \tfrac{1}{2} \hat{P}^{\pm\omega} \hat{P}^{ABCD} \{ & \tfrac{1}{4} (\eta^{CD}(\omega_C, \omega_D) \\ & + \tfrac{1}{2} \boldsymbol{F} t^{CD}(\omega_C, \omega_D)) t^{AB}(\omega_A, \omega_B) \\ & + \tfrac{1}{6} \overline{t^A}(\omega_A) \boldsymbol{C} t^B(\omega_B) t^C(\omega_C) t^D(\omega_D) \\ & + \tfrac{1}{24} \boldsymbol{H} t^A(\omega_A) t^B(\omega_B) t^C(\omega_C) t^D(\omega_D) \\ & + \tfrac{1}{2} \overline{t^A}(\omega_A) \boldsymbol{B}^B t^C(\omega_C) t^D(\omega_D) \} \end{aligned} \quad (20)$$

with

$$\eta^{CD} = \hat{P}^{CD} (\tfrac{1}{2} \boldsymbol{G} t^C(\omega_C) t^D(\omega_D) + \boldsymbol{F}^C t^D(\omega_D) + \overline{t^C}(\omega_C) \boldsymbol{B} t^D(\omega_D) + \overline{t^C}(\omega_C) \boldsymbol{A}^D), \quad (21)$$

$$\boldsymbol{G}_{\mu\nu\gamma} = \left(\frac{\partial^3 L}{\partial t_\mu \partial t_\nu \partial t_\gamma} \right)_0, \quad (22)$$

$$\boldsymbol{H}_{\mu\nu\gamma\delta} = \left(\frac{\partial^4 L}{\partial t_\mu \partial t_\nu \partial t_\gamma \partial t_\delta} \right)_0, \quad (23)$$

$$\boldsymbol{C}_{\mu\nu\gamma\delta} = \left(\frac{\partial^4 L}{\partial \overline{t}_\mu \partial t_\nu \partial t_\gamma \partial t_\delta} \right)_0, \quad (24)$$

$$\boldsymbol{B}^A_{\mu\nu\gamma} = \left(\frac{\partial^4 L}{\partial \epsilon_A(\omega_A) \partial \overline{t}_\mu \partial t_\nu \partial t_\gamma} \right)_0. \quad (25)$$

The operator $\hat{P}^{\pm\omega}$ symmetrizes with respect to an overall sign inversion of the frequency arguments and simultaneous complex conjugation. The implementation of the cubic response functions for the coupled cluster models CCS, CC2 and CCSD has been reported in Ref. 17. The quasienergy and the time-dependent cluster equations for the coupled cluster methods CCS and CCSD are obtained by truncating the cluster operator after the single and double excitation level, respectively. In the CC2 method the equations for the double excitation amplitudes are approximated by the lowest order terms.[26]

In the static limit the coupled cluster response calculations become equivalent to finite field calculations where the external perturbation is first applied after the SCF calculation. For a two-electron system the CCSD response approach becomes equivalent to a FCI calculation.

The computational most demanding part in the coupled cluster response calculations is the solution of the linear equations for the cluster amplitude and Lagrangian multiplier responses. For frequency-dependent second hyperpolarizabilities $\gamma_{X_0 X_1 X_2 X_3}(\omega_0; \omega_1, \omega_2, \omega_3)$ one must solve for each operator/frequency pair (X_i, ω_i) the first-order response equations for $t^{X_i}(\omega_i)$, $t^{X_i}(-\omega_i)$, $\overline{t^{X_i}}(\omega_i)$, and $\overline{t^{X_i}}(-\omega_i)$ and for each combination of these pairs the second-order response equations for $t^{X_i X_j}(\omega_i, \omega_j)$ and $t^{X_i X_j}(-\omega_i, -\omega_j)$. The number of response equations that actually has to be solved varies strongly with the optical proccesses and the tensor components that have to be calculated. In general it is advantageous to calculate the hyperpolarizabilities for several optical proccesses and several tensor components at one time.

III. COMPUTATIONAL DETAILS

For the four optical proccesses we shall consider, the frequency arguments of the second hyperpolarizability are conventionally defined as[5] $\gamma^{\mathrm{dcKerr}}_{\mu\nu\eta\xi}(\omega) = \gamma_{\mu\nu\eta\xi}(-\omega; 0, 0, \omega)$, $\gamma^{\mathrm{DFWM}}_{\mu\nu\eta\xi}(\omega) = \gamma_{\mu\nu\eta\xi}(-\omega; \omega, \omega, -\omega)$, $\gamma^{\mathrm{ESHG}}_{\mu\nu\eta\xi}(\omega) = \gamma_{\mu\nu\eta\xi}(-2\omega; \omega, \omega, 0)$, and $\gamma^{\mathrm{THG}}_{\mu\nu\eta\xi}(\omega) = \gamma_{\mu\nu\eta\xi}(-3\omega; \omega, \omega, \omega)$. Note that for each of these hyperpolarizabilities the second and the third frequency argument are the same and that the hyperpolarizabilities therefore are symmetric in the second and third index, ν and η.

In most ESHG and THG experiments the measured tensor component is the isotropic average:[5]

$$\gamma_{||} = \frac{1}{15} \sum_{\xi\eta} (\gamma_{\xi\xi\eta\eta} + \gamma_{\xi\eta\eta\xi} + \gamma_{\xi\eta\xi\eta}), \quad \xi, \eta = x, y, z. \quad (26)$$

Only few ESHG experiments exist for the ''perpendicular'' isotropic tensor component:[5,34]

$$\gamma_{\perp} = \frac{1}{15} \sum_{\xi\eta} (2\gamma_{\xi\eta\eta\xi} - \gamma_{\xi\xi\eta\eta}), \quad \xi, \eta = x, y, z. \quad (27)$$

For the dc Kerr effect the tensor component relevant for comparison with experiment is:[5]

$$\gamma_K = \frac{3}{2} (\gamma_{||} - \gamma_{\perp}). \quad (28)$$

For atoms $\gamma_{xxzz} + \gamma_{xzzx} + \gamma_{xzxz} = \gamma_{zzzz}$ and therefore $\gamma_{||} = \gamma_{zzzz}$ and $\gamma_{\perp} = \gamma_{zxxz}$ and the Kerr hyperpolarizability becomes $\gamma_K = 3/2(\gamma_{zzzz} - \gamma_{zxxz})$. For spherical top molecules (3 equivalent principal axes) $\gamma_{||}$ and $\gamma_{\perp}$ become:

$$\gamma_{||} = \tfrac{3}{5}\gamma_{zzzz} + \tfrac{2}{5}\gamma_{xxzz} + \tfrac{2}{5}\gamma_{zxxz} + \tfrac{2}{5}\gamma_{xzxz}, \quad (29)$$

$$\gamma_{\perp} = \tfrac{1}{5}\gamma_{zzzz} + \tfrac{4}{5}\gamma_{zxxz} - \tfrac{2}{5}\gamma_{xxzz}. \quad (30)$$

Using that for linear molecules $\gamma_{xxyy}+\gamma_{xyyx}+\gamma_{xyxy} = \gamma_{xxxx}$, the tensor components $\gamma_{||}$ and $\gamma_{\perp}$ can be reduced to:

$$\gamma_{||} = \tfrac{1}{15}(8\gamma_{xxxx} + 2\gamma_{xxzz} + 2\gamma_{zzxx} + 2\gamma_{zxxz} + 2\gamma_{xzzx} + 2\gamma_{xzxz} + 2\gamma_{zxzx} + 3\gamma_{zzzz}), \quad (31)$$

$$\gamma_{\perp} = \tfrac{1}{15}(\gamma_{xxxx} + 5\gamma_{xyyx} + 4\gamma_{zxxz} - 2\gamma_{xxzz} + 4\gamma_{xzzx} - 2\gamma_{zzxx} + \gamma_{zzzz}). \quad (32)$$

Independent of the spatial symmetry of the molecule or atom, the isotropic components $\gamma_{||}$, $\gamma_{\perp}$, and γ_K become in the static limit $\gamma_{||} = 3\gamma_{\perp} = \gamma_K = \gamma_0$.

In the single point calculations for N_2 and CH_4 we used the equilibrium internuclear distances $r_{NN} = 2.074$ a.u. and $r_{CH} = 2.052$ a.u.[35,36] In the CCS, CC2 and CCSD response calculations for Ne, Ar, and CH_4 we have, if not stated otherwise, used a frozen core approximation. For the individual systems we have frozen the following orbital occupations: Ne: $1s^2$, Ar: $1s^2 2s^2 2p^6$, CH_4: $1a_1^2$. No frozen core approximation was used for N_2 or in the SCF calculations. For the SCF hyperpolarizability calculations we employed the cubic response function implementation[37] in the DALTON program package.[38] In all calculations we used the correlation consistent basis sets developed by Dunning and co-workers.[29,39–42] Several basis sets were used for the calculation of static hyperpolarizabilities (see Sec. IV), but all frequency-dependent hyperpolarizabilities were calculated using for Ne and Ar the t-aug-cc-pV5Z and for N_2 and CH_4 the t-aug-cc-pVTZ basis sets. Orbital relaxed CCSD and CCSD(T) finite field calculations were performed using the t-aug-cc-pV5Z basis sets for Ne and Ar and the d-aug-cc-pVTZ sets for N_2 and CH_4. For Neon CCSD and CCSD(T) calculations were also done in the t-aug-cc-pCV5Z basis.

IV. BASIS SET INVESTIGATION

In Tables I and II we have listed the results of a basis set study at the SCF and the CCSD response level. We have employed the series of correlation consistent basis sets x-aug-cc-pVXZ proposed by Woon and Dunning.[29] For each fixed x-aug level these basis sets converge to a valence basis set limit, if the XZ level is increased successively; to obtain convergence to the complete basis set limit also additional core orbitals must be included by means of the x-aug-cc-pCVXZ series. If for a fixed XZ level the augmentation x is increased the results converge to a series limit which is different from the basis set limit. In particular for the second hyperpolarizabilities of atoms and linear molecules it is well known that f functions are crucial already at the SCF level and thus accurate results cannot be expected from the double-zeta basis sets x-aug-cc-pVDZ. For molecules with a two- or three-dimensional structure f functions are less important for γ_0. As was found by Woon and Dunning in an earlier basis set study,[29] polarizabilities and hyperpolarizabilities converge slowly in XZ, if the augmentation level is low, reflecting the important role of diffuse functions for these properties. For Ne and Ar we obtain both at the Hartree-Fock level and in the CCSD response calculations an acceptable convergence in the triply-augmented series. The fourth set of augmentation functions improves slightly the convergence, although in the correlated calculations an increase of the cardinal number X becomes at the triply-augmented level more important than augmentation with diffuse functions. For the diatomic molecule N_2 the convergence with the basis sets is somewhat faster than for the rare gas atoms. For N_2 already in the doubly-augmented series an increase of the cardinal number X is of the same

TABLE I. Static isotropic hyperpolarizabilities γ_0 at the Hartree-Fock level as a function of the basis set.

	Ne	Ar	N_2	CH_4
aug-cc-pVDZ	20.34	296.0	456.0	1497.4
aug-cc-pVTZ	28.31	456.4	560.0	1745.1
aug-cc-pVQZ	38.61	685.4	654.2	1830.0
aug-cc-pV5Z	50.14	741.0	684.5	⋯
d-aug-cc-pVDZ	49.29	717.5	672.0	1773.8
d-aug-cc-pVTZ	57.27	841.3	697.1	1868.3
d-aug-cc-pVQZ	62.03	889.7	709.9	1863.5
d-aug-cc-pV5Z	67.53	944.0	713.9	⋯
t-aug-cc-pVDZ	53.22	704.1	669.2	1815.3
t-aug-cc-pVTZ	66.54	941.2	710.1	1869.4
t-aug-cc-pVQZ	67.80	947.2	713.2	1867.5
t-aug-cc-pV5Z	68.64	961.0	⋯	⋯
q-aug-cc-pVDZ	53.27	705.6	679.7	1816.4
q-aug-cc-pVTZ	68.85	946.5	716.9	1870.5
q-aug-cc-pVQZ	68.50	953.0	714.9	⋯
q-aug-cc-pV5Z	68.66	961.4	⋯	⋯
Numerical HF [a]	69.3	966	⋯	⋯

[a]Reference 63.

TABLE II. Static isotropic hyperpolarizabilities γ_0 at the CCSD level as a function of the basis set.

	Ne	Ar	N_2	CH_4
aug-cc-pVDZ	29.6	375.5	684.4	1931.3
aug-cc-pVTZ	42.2	579.4	745.1	2198.9
aug-cc-pVQZ	58.5	853.8	822.0	2285.0
aug-cc-pV5Z	76.8	914.0	844.1	⋯
d-aug-cc-pVDZ	83.9	990.1	937.6	2327.6
d-aug-cc-pVTZ	94.2	1092.1	895.3	2363.5
d-aug-cc-pVQZ	100.2	1110.4	880.7	2329.6
d-aug-cc-pV5Z	108.0	1158.5	873.2	⋯
t-aug-cc-pVDZ	94.4	974.8	935.4	2378.2
t-aug-cc-pVTZ	110.3	1218.4	903.0	2364.8
t-aug-cc-pVQZ	110.0	1178.9	882.7	⋯
t-aug-cc-pV5Z	110.2	1178.5	⋯	⋯
q-aug-cc-pVDZ	94.5	975.5	943.4	2380.3
q-aug-cc-pVTZ	114.5	1225.5	908.8	⋯
q-aug-cc-pVQZ	111.2	1185.9	⋯	⋯
q-aug-cc-pV5Z	110.2	1179.0	⋯	⋯

importance as the inclusion of a third augmentation level. Also for methane we find good convergence: At the SCF level the effects of going from the d-aug-cc-pVTZ basis to the next higher XZ or x-aug are small.

At the Hartree-Fock level the hyperpolarizability usually increases both, if x-aug or XZ is increased. For the correlation contribution to the hyperpolarizability the convergence pattern is dominated by different effects: In the CCSD response calculations an increase of γ_0 with the cardinal number X is only found for the lower augmentation levels. We find beyond singly-augmentation for N_2 and CH_4 and beyond doubly-augmentation for Ne and Ar a decrease of the hyperpolarizability if the correlation of the valence orbitals is improved in the series pVTZ – pVQZ – pV5Z. In particular for N_2 and CH_4, the correlation contribution to γ_0 is not much affected by the x-aug level, but decreases considerably if the correlation of the valence orbitals is improved by increasing XZ. Many correlated hyperpolarizability calculations in the literature were performed with basis sets of triple-zeta or similar quality and basis set convergence was often only explored with respect to augmentation with diffuse functions. From the above observation one may conclude that many of these studies obtained too large results for γ and underestimated the remaining basis set errors.

For neon and argon the SCF basis set limit is known from numerical Hartree-Fock calculations (see Table I). With the t-aug-cc-pV5Z basis sets, which are used in the subsequent frequency-dependent calculations, the remaining basis set errors in the Hartree-Fock calculations are 0.7% (Ne) and 0.5% (Ar). At the CCSD response level these basis sets give $\gamma_0 = 110.2$ a.u. for Ne and $\gamma_0 = 1178.5$ a.u. for Ar, when the core orbitals are frozen. With all electrons correlated and polarized,[43] the results in the same basis sets are $\gamma_0^{\mathrm{Ne}} = 109.3$ a.u. and $\gamma_0^{\mathrm{Ar}} = 1172$ a.u. (see Table III). For neon we did also a CCSD response calculation with all electrons correlated in the corresponding core-valence basis, t-aug-cc-pCV5Z, but the additional core orbitals have only a minor effect on the hyperpolarizability: $\gamma_0^{\mathrm{Ne}} = 108.9$ a.u. Because of the slower convergence of the correlated calculations the remaining basis set errors in the t-aug-cc-pV5Z basis should at the CCSD response level be somewhat larger than in the Hartree-Fock calculations, likely in the range of 1%–3%. For N_2 and CH_4 we estimate, based on the calculations in the largest basis sets, the Hartree-Fock limit at the equilibrium geometries for γ_0 as 715 ± 2 a.u. and 1865 ± 5 a.u., respectively. For the subsequent frequency-dependent calculations we used for both molecules the t-aug-cc-pVTZ basis sets. At the CCSD response level this basis gives $\gamma_0 = 903.0$ a.u. for N_2 and $\gamma_0 = 2364.8$ a.u. for CH_4, where for the latter molecule the $1a_1^2$ orbital occupation was kept frozen. In the corresponding core-valence sets, t-aug-cc-pCVTZ, we obtained with all electrons correlated $\gamma_0^{\mathrm{N_2}} = 896.3$ a.u. and $\gamma_0^{\mathrm{CH_4}} = 2353$ a.u., corresponding to core effects of -6.7 a.u. for N_2 and -12 a.u. for CH_4. To obtain estimates for the remaining basis set errors at the correlated level, we did for the static hyperpolarizabilities some CCSD response calculations with larger basis sets. For the N_2 molecule the largest basis set we have used is the d-aug-cc-pV5Z basis, consisting of a $[8s7p6d5f4g3h]$ contraction with 326 basis functions.

TABLE III. Static isotropic hyperpolarizabilities γ_0 obtained at different levels of the coupled cluster hierarchies and with and without the inclusion of core correlation effects.

	Ne	Ar	N_2	CH_4
CCS unrelaxed	78.2[a]	1154.[a]	824.9[b]	2228.[b]
CC2 unrelaxed	135.8[a]	1247.[a]	991.9[b]	2557.[b]
CCSD unrelaxed	110.2[a]	1178.[a]	903.0[b]	2365.[b]
			895.3[c]	2364.[c]
SCF	68.6[a]	961.[a]	710.1[b]	1869.[b]
CCSD relaxed	99.1[a]	1106.[a]	853.6[c]	2176.[c]
CCSD relaxation effect [d]	−11.1[a]	−72.[a]	−41.7[c]	−188.[c]
CCSD(T) rel.	107.8[a]	1168.[a]	910.7[c]	2294.[c]
relaxation and triples effect [e]	−2.4[a]	−10.[a]	15.4[c]	−70.[c]
CCSD resp. core corr. [f]	108.9	1172.	896.3	2353.
CCSD(T) core corr. [g]	107.1	1159.		
core correlation effect [h]	−0.6	−9.	−6.7	−12.
MCSCF [i]	106.	1123.	885.	2152.
CCSD(T) [j]	110.3	1231.	1010.	2370.
CCSD(T)-R12 [k]	104.7			
QCISD(T) [l]			946.	

[a]t-aug-cc-pV5Z basis.
[b]t-aug-cc-pVTZ basis.
[c]d-aug-cc-pVTZ basis.
[d]Difference between relaxed CCSD and unrelaxed CCSD results.
[e]Difference between relaxed CCSD(T) and unrelaxed CCSD results.
[f]CCSD resp. all electrons correlated; the basis sets are: Ne: t-aug-cc-pCV5Z, Ar: t-aug-cc-pV5Z, N_2: t-aug-cc-pCVTZ, CH_4: t-aug-cc-pCVTZ.
[g]CCSD(T), all electrons correlated; basis sets: t-aug-cc-pCV5Z for Ne and t-aug-cc-pV5Z for Ar.
[h]Ne, Ar: from the CCSD(T) calculations; N_2, CH_4: from the CCSD response calculations.
[i]Ne: Ref. 11; Ar: Ref. 64; N_2: Ref. 65; CH_4: Ref. 59.
[j]Ne: Ref. 10; Ar: Ref. 9; N_2: Ref. 66; CH_4: Ref. 67.
[k]Reference 68.
[l]Reference 69.

At the CCSD response level this basis set gives $\gamma_0 = 873.2$ a.u. Adding to this result the core correction of -6.7 a.u., we obtain a best estimate for the unrelaxed CCSD basis set limit of 867 ± 7 a.u. for the static second hyperpolarizability of N_2 at the equilibrium distance $r_e = 2.074$ a.u. For methane the largest basis set we have used is the d-aug-cc-pVQZ basis which consists of a $(14s8p5d4f3g)/[7s6p5d4f3g]$ contraction at the carbon atom and a $(8s5p4d3f)/[6s5p4d3f]$ contraction at the hydrogen atom, giving in total 353 basis functions. This basis set gives at the CCSD response level for the static second hyperpolarizability of the methane molecule a result of 2329.6 a.u. Adding the estimate for the core effect obtained with the t-aug-cc-pVTZ and t-aug-cc-pCVTZ basis sets (-12 a.u.), we obtain for the CCSD unrelaxed basis set limit of the static second hyperpolarizability of CH_4 a best estimate of 2318 ± 35 a.u.

V. COMPARISON OF DIFFERENT WAVE FUNCTION MODELS

In the coupled cluster response approach the nonrelaxed Hartree-Fock wave function of the unperturbed system is

TABLE IV. Third harmonic generation hyperpolarizabilities $\gamma_{||}(-3\omega;\omega,\omega,\omega)$ for Ne. Comparision of SCF, CCS, CC2 and CCSD dispersion curves for the q-aug-cc-pV5Z basis.

λ/nm	ω/a.u.	SCF	CCS	CC2	CCSD
1319.0	0.034544	70.95	80.71	141.7	114.6
1055.0	0.043188	72.30	82.18	145.1	117.2
694.3	0.065625	77.57	87.90	159.0	127.4
632.8	0.072003	79.61	90.11	164.5	131.5
590.0	0.077226	81.49	92.15	169.6	135.2
514.5	0.088558	86.31	97.37	183.0	144.9
488.0	0.093368	88.71	99.96	189.8	149.8

TABLE VI. Third harmonic generation hyperpolarizabilities $\gamma_{||}(-3\omega;\omega,\omega,\omega)$ for N_2 at the equilibrium bond distance $R_{NN}=2.074$ bohr. Comparision of SCF, CCS, CC2 and CCSD dispersion curves for the t-aug-cc-pVTZ basis.

λ/nm	ω/a.u.	SCF	CCS	CC2	CCSD
1055.0	0.043188	795.8	919.0	1127.5	1020.7
694.3	0.065625	932.8	1068.1	1350.9	1212.2
632.8	0.072003	990.6	1130.6	1447.6	1294.2
590.0	0.077226	1046.4	1190.8	1542.6	1374.2
514.5	0.088558	1201.8	1357.6	1814.4	1600.5
488.0	0.093368	1286.2	1447.6	1966.7	1725.5
457.9	0.099505	1415.2	1584.7	2206.4	1919.9

used as reference state in the coupled cluster calculation. In the static limit this becomes equivalent to finite field calculations where the external perturbation is first included in the Hamiltonian after the SCF step. Alternatively, in the orbital-relaxed coupled cluster approach the perturbation is already included in the SCF step. In orbital-relaxed CCS calculations the cluster amplitudes become zero and therefore the CCS ground state energy and properties become equal to the SCF results. For frequency-dependent properties the explicit treatment of orbital relaxation would lead to artificial poles in the correlated results for frequencies at which the SCF response functions become singular. However, in the static limit both, the nonrelaxed coupled cluster response hierarchy CCS, CC2, CCSD, etc., and orbital-relaxed hierarchy SCF, CC2, CCSD, etc., are applicable and both hierachies converge in the limit of a complete cluster expansion to the full CI treatment. The question arises, how efficient orbital relaxation can be treated implicitly by the single excitation manifold of the cluster operator. In the literature it is usually assumed that the orbital-relaxed hierarchy is more reliable. Numerical investigations[44,45] of this aspect, however, did not find a significant better performance of orbital-relaxed calculations compared to nonrelaxed ones.

In order to compare the performance of the two coupled cluster hierachies for the hyperpolarizabilities we have calculated the static limit values, γ_0, for our four systems, using the unrelaxed CCS, CC2 and CCSD response approaches and the orbital-relaxed SCF, CCSD and CCSD(T) models (see Table III). The first elements in the two hierachies, nonrelaxed CCS and orbital-relaxed SCF, give for the present examples results of similar accuracy, with the CCS values for all four systems between the SCF and the CCSD results; for Ne and N_2 closer to SCF and for Ar and CH_4 closer to CCSD. This indicates that orbital relaxation can efficiently be treated implicitly by the single excitation manifold of the cluster operator.

From SCF to CCSD(T) the results for γ_0 increase by $\approx$60% for Ne and by 20%–30% for Ar, N_2, and CH_4, reflecting the well-known large effects of dynamic electron correlation on the magnitude of γ_0. If we compare unrelaxed CC2 with the CCSD and CCSD(T) calculations, we find that the CC2 response approach overshoots the correlation contribution significantly for all four examples. In the static limit CC2 is almost no improvement upon CCS. For all four examples the difference between unrelaxed CCSD and orbital-relaxed CCSD(T) values is only a small effect: Ne: 2.2%, Ar: 0.8%, N_2: 1.7% and CH_4: 3.1%. The difference between orbital-relaxed CCSD and CCSD(T) results is much larger: Ne: 8.8%, Ar: 5.6%, N_2: 6.7% and CH_4: 8.2%. If one assumes that the orbital-relaxed CCSD(T) values are close to the full CI limit, one thus finds that the remaining correlation error for the hyperpolarizabilities are larger in the orbital-relaxed CCSD calculations than in the unrelaxed CCSD response approach. From the present results there is no reason to expect improvements by treating orbital relaxation explicitly in hyperpolarizability calculations with coupled cluster wave functions.

To compare the description of the dispersion in SCF, CCS, CC2 and CCSD, we give in Tables IV–VII results for the third harmonic generation hyperpolarizabilities for Ne, Ar, N_2 and CH_4. In the literature it has been speculated that the dispersion contribution to the hyperpolarizabilities might be less sensitive to basis set selection and electron correlation treatment than the static hyperpolarizabilities.[4,5] This suspection was based on a comparison of results obtained

TABLE V. Third harmonic generation hyperpolarizabilities $\gamma_{||}(-3\omega;\omega,\omega,\omega)$ for Ar. Comparision of SCF, CCS, CC2 and CCSD dispersion curves for the q-aug-cc-pV5Z basis.

λ/nm	ω/a.u.	SCF	CCS	CC2	CCSD
1319.0	0.034544	1042.1	1246.3	1358.5	1282
1055.0	0.043188	1092.2	1303.2	1427.5	1346
694.3	0.065625	1308.0	1547.0	1727.8	1626
632.8	0.072003	1401.3	1652.0	1859.3	1748
590.0	0.077226	1492.9	1754.7	1989.2	1869
514.5	0.088558	1755.0	2047.7	2366.2	2217
488.0	0.093368	1901.9	2211.4	2581.0	2416

TABLE VII. Third harmonic generation hyperpolarizabilities $\gamma_{||}(-3\omega;\omega,\omega,\omega)$ for CH_4 at the equilibrium geometry, $r_{CH}=2.052$ a.u. Comparision of SCF, CCS, CC2 and CCSD dispersion curves for the t-aug-cc-pVTZ basis.

λ/nm	ω/a.u.	SCF	CCS	CC2	CCSD
1319.0	0.034544	2071.7	2456.9	2854.7	2635.2
1064.0	0.042823	2193.7	2594.2	3035.7	2799.2
671.5	0.067853	2864.6	3344.5	4051.5	3716.0
589.0	0.077357	3318.9	3848.3	4758.5	4350.7
514.5	0.088559	4126.5	4738.0	6055.4	5507.8
476.5	0.095621	4888.8	5571.9	7328.7	6635.7

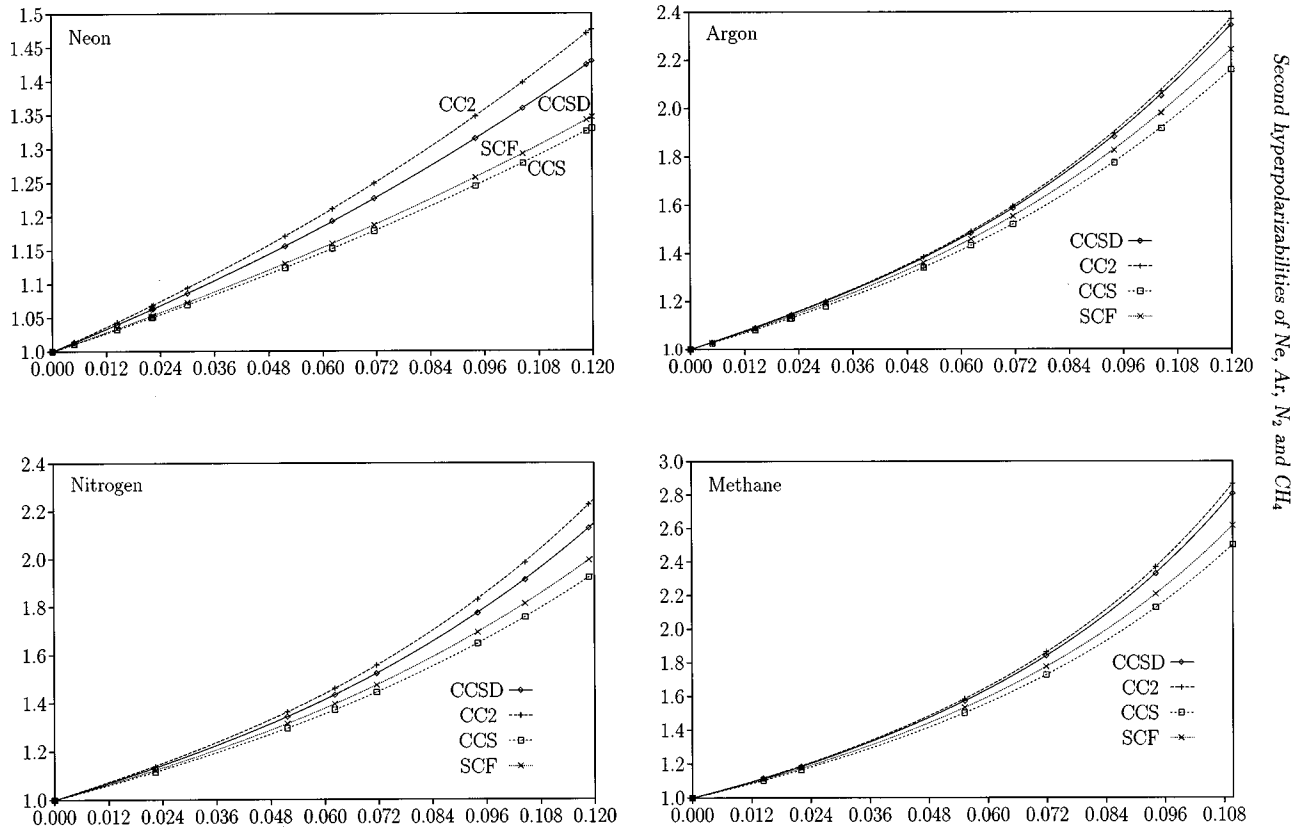


FIG. 1. Comparison of the relative dispersion $\gamma_{||}(\omega)/\gamma_{||}(0)$ in the SCF (RPA) and the CCS, CC2 and CCSD response approaches for the third harmonic generation in Ne, Ar, N_2 and CH_4.

from SCF, MCSCF and MP2 calculations. However, the curvature of the dispersion curves is sensitive to the position of the first pole in $\gamma(\omega)$ and is thus sensitive to the lowest excitation energy. As the MP2 frequency-dependent properties have their lowest pole at the same position as in SCF,[23,46] it is not surprising that the MP2 dispersion is usually similar to the SCF dispersion. In Fig. 1 we have for Ne, Ar, N_2, and CH_4 plotted the ratio $\gamma_{||}^{\mathrm{THG}}(\omega)/\gamma_0$ at the SCF and the CCS, CC2 and CCSD response level. From these plots it is obvious that dynamic correlation has as large effects on the dispersion of the hyperpolarizabilities as it has on the static hyperpolarizabilities. For all four molecules the dispersion of γ is strongly underestimated by the uncorrelated SCF and CCS methods, which give very similar results for the dispersion. Despite the disappointing performance of CC2 for the absolute magnitude of γ, the relative dispersion effect $\gamma_{||}^{\mathrm{THG}}(\omega)/\gamma_0$ is at the CC2 level significantly better than at the CCS or SCF level.

VI. COMPARISION WITH EXPERIMENT

A. Neon and argon

In Tables VIII and IX we list for Ne and Ar the results of CCSD response calculations for the dc Kerr effect, DFWM, ESHG and THG in the frequency range $\omega=0.0-0.1$ a.u. or $\lambda=455.6$ nm$-\infty$. The CCSD dispersion curves for the four optical processes are shown in Fig. 2. The electric field induced second harmonic generation (ESHG) is of particular interest, because for this process accurate experimental data are available from the work of Shelton and co-workers,[1–5] covering the broad range of wavelengths between 1319 nm and 457.9 nm. Detailed plots for ESHG in Ne and Ar are shown in Figs. 3 and 4. The ESHG hyperpolarizability of Ne and its static limiting value has been the subject of numerous *ab initio* calculations and several experimental investigations. The ''ups'' and ''downs'' of the theoretical and experimental estimates for γ_0^{Ne} can be found in recent reviews by Bishop[47] and Shelton and Rice.[5] After the latest reinvestigation by Shelton and Donley,[4] ESHG measurements at four frequencies were presumed to be accurate within $\pm 0.4-0.8$ a.u. A fit of these four points to $\gamma_{||}^{\mathrm{ESHG}}(\omega)=\gamma_0(1+6A\omega^2+36B\omega^4)$, where B was constraint to 5.50 a.u. [a value arbitrarily chosen between the results of a MP2 (Refs.

TABLE VIII. Dispersion curves for different optical processes for $\gamma_{||}$ of Ne, calculated at the CCSD level using the t-aug-cc-pV5Z basis.

λ/nm	ω/a.u.	Kerr [a]	DFWM	ESHG	THG
1319.0	0.034544	110.9	111.6	112.4	114.6
1064.0	0.042823	111.3	112.4	113.6	117.1
1055.0	0.043188	111.3	112.5	113.6	117.2
694.3	0.065625	112.8	115.5	118.3	127.4
632.8	0.072003	113.4	116.7	120.1	131.5
590.0	0.077226	113.9	117.7	121.7	135.2
514.5	0.088558	115.0	120.2	125.7	144.9
488.0	0.093368	115.6	121.4	127.7	149.8
457.9	0.099505	116.4	123.1	130.4	156.9

[a]For the Kerr process the table lists γ_K. For the definition of γ_K see Sec. III.

TABLE IX. Dispersion curves for different optical processes for $\gamma_{||}$ of Ar, calculated at the CCSD level using the t-aug-cc-pV5Z basis.

λ/nm	ω/a.u.	Kerr [a]	DFWM	ESHG	THG
1319.0	0.034544	1195	1212	1229	1282
1064.0	0.042823	1204	1230	1257	1343
1055.0	0.043188	1204	1231	1258	1346
694.3	0.065625	1239	1305	1376	1626
632.8	0.072003	1252	1334	1422	1748
590.0	0.077226	1264	1360	1465	1869
514.5	0.088558	1293	1426	1577	2217
488.0	0.093368	1307	1458	1634	2416

[a]For the dc Kerr effect the table lists γ_K. For the definition of γ_K see Sec. III.

48,10) and a CASSCF (Ref. 49) calculation] led to the estimate for the static limiting value $\gamma_0^{\mathrm{Ne}}=108.1\pm2.2$ a.u. However, the dispersion curve obtained by this fit does not overlap with the error bars of the two ESHG measurements in the infrared at 1319 nm and 1064 nm, as is seen in Fig. 3. Thus, at least one of these two measurements must have a larger inaccuracy than indicated by its statistical uncertainty. Because of the difficulties to extrapolate from the experimental data to the static limit based on a fitted dispersion function, we suggested recently[50] to use the dispersion curve from a CCSD response calculation, shifted such that it matches the two points measured in the visible to extrapolate to the static limit. This extrapolation leads to the refined estimate $\gamma_0^{\mathrm{Ne}}=106.4\pm2$ a.u. Furthermore it showed that the ESHG experiment at 1056 nm is in good agreement with the CCSD dispersion curve and the ESHG experiments at 514.5 and 488.0 nm, but that the value measured at 1319 nm is too large by ≈2.4 a.u. The refined estimate for γ_0^{Ne} differs from the static CCSD response result by 3.8 a.u. However, this result was obtained using a frozen core approximation and the t-aug-cc-pV5Z basis. If the core electrons are correlated and the effects of connected triples are included by means of a CCSD(T) finite field calculation, one obtains for the static hyperpolarizability of neon $\gamma_0^{\mathrm{Ne}}=107.1$ a.u. (cmp. Table III), in good agreement with the refined experimental estimate. If we account for these small additional basis sets and correlation effects by a multiplicative correction $\gamma_{||}^{\mathrm{est}}(\omega)=\gamma_{\text{t-aug-cc-pV5Z}}^{\text{CCSD resp}}(\omega)\times\gamma_{\text{t-aug-cc-pVC5Z}}^{\text{CCSD(T)}}(0)/\gamma_{\text{t-aug-cc-pV5Z}}^{\text{CCSD resp}}(0)$, we get at the wavelengths of the three most reliable ESHG points: $\gamma_{||}^{\mathrm{est}}(488.0\,\mathrm{nm})=124.1$ a.u., $\gamma_{||}^{\mathrm{est}}(514.5\,\mathrm{nm})=122.2$ a.u. and $\gamma_{||}^{\mathrm{est}}(1064\,\mathrm{nm})=110.4$ a.u. These results agree within 0.5% with the experimental ESHG data (see Table X). Agreement between theory and experiment within a 1% range was before only achieved for the two-electron system He and H_2.[5,7] We note that based on the study in Sec. IV remaining basis set effects can be expected to lower the final results. The remaining correlation effects (iterative triples and connected higher excitations) will in the orbital relaxed approach likely increase γ_0 slightly. Each of these effects might change γ_0^{Ne} by 1–3 a.u. Thus, despite a better

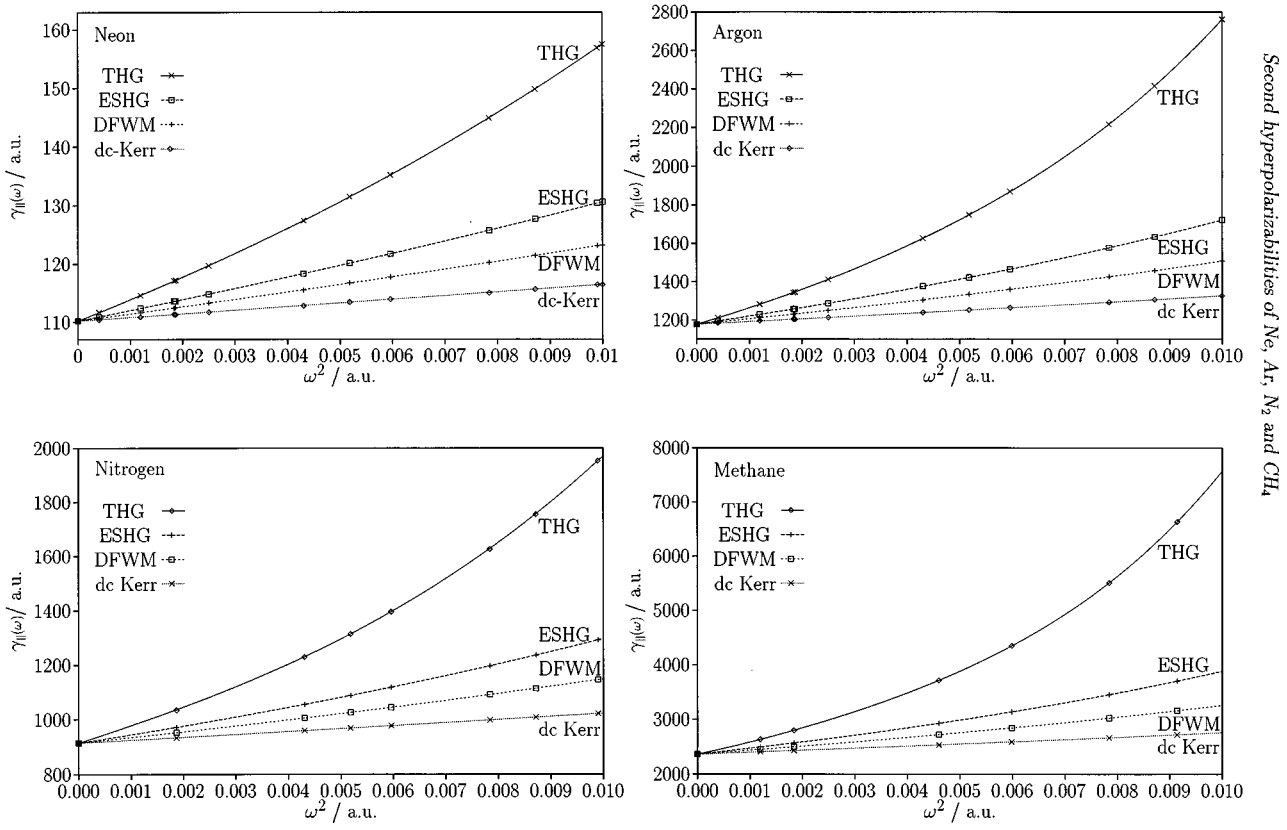


FIG. 2. Dispersion curves for the dc Kerr effect, DFWM, ESHG and THG in Ne, Ar, N_2 and CH_4 (CCSD response; Ne: t-aug-cc-pV5Z basis, $1s^2$ frozen; Ar: t-aug-cc-pV5Z basis, $1s^22s^22p^6$ frozen; N_2: t-aug-cc-pVTZ basis, no frozen core; CH_4: t-aug-cc-pVTZ basis, $1a_1^2$ frozen).

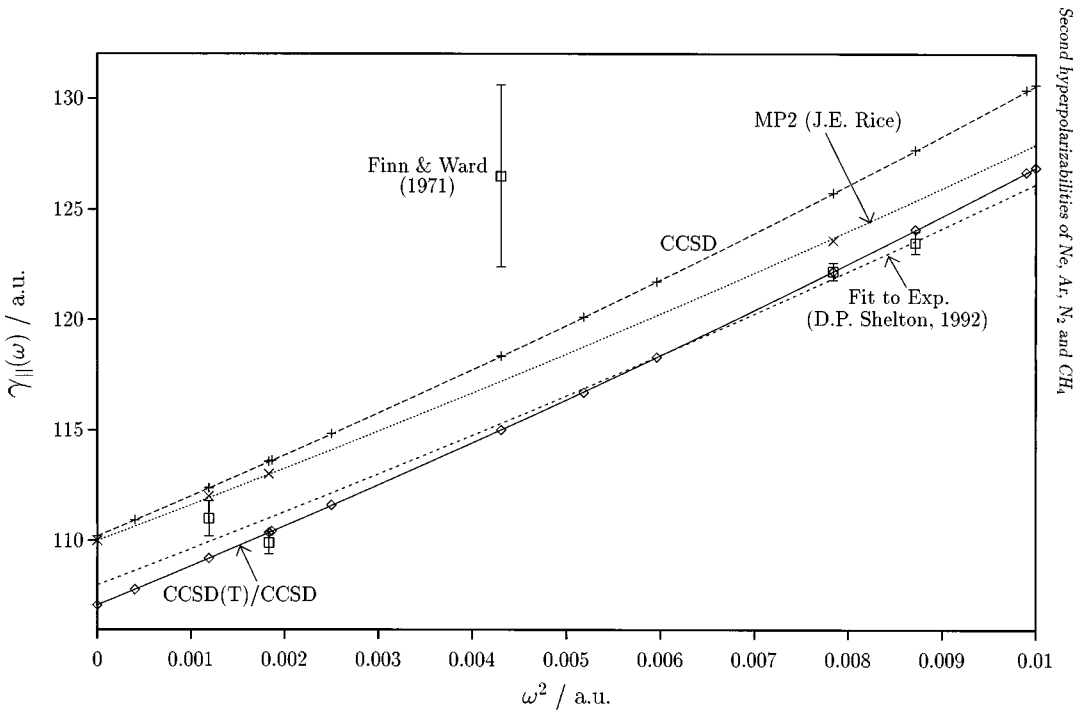


FIG. 3. Electric field induced second harmonic generation in neon. Comparison of the CCSD and the CCSD(T)/CCSD response curves with the experimental results (Refs. 3,4,71) and the CCSD(T)/MP2 dispersion curve of Rice (Refs. 5,10,48).

agreement with the experimental values one must estimate the remaining intrinsic uncertainity of the *ab initio* results as about ± 3 a.u.

For argon the experimental situation is more favorable than for neon, since accurate ESHG data are available for more that 20 frequencies in the range $\lambda = 457.9-1319$ nm. The CCSD dispersion curve was obtained with the t-aug-cc-pV5Z basis and with only the valence electrons correlated. Even though connected triples and core effects are not considered it is already close to the fit of the experimental ESHG data. The CCSD response result for γ_0^{Ar} is within the uncertainity of the result extrapolated from a fit to this data. Correlating in the t-aug-cc-pV5Z basis all electrons give in a CCSD response calculation $\gamma_0^{\mathrm{Ar}} = 1172$ a.u. and in

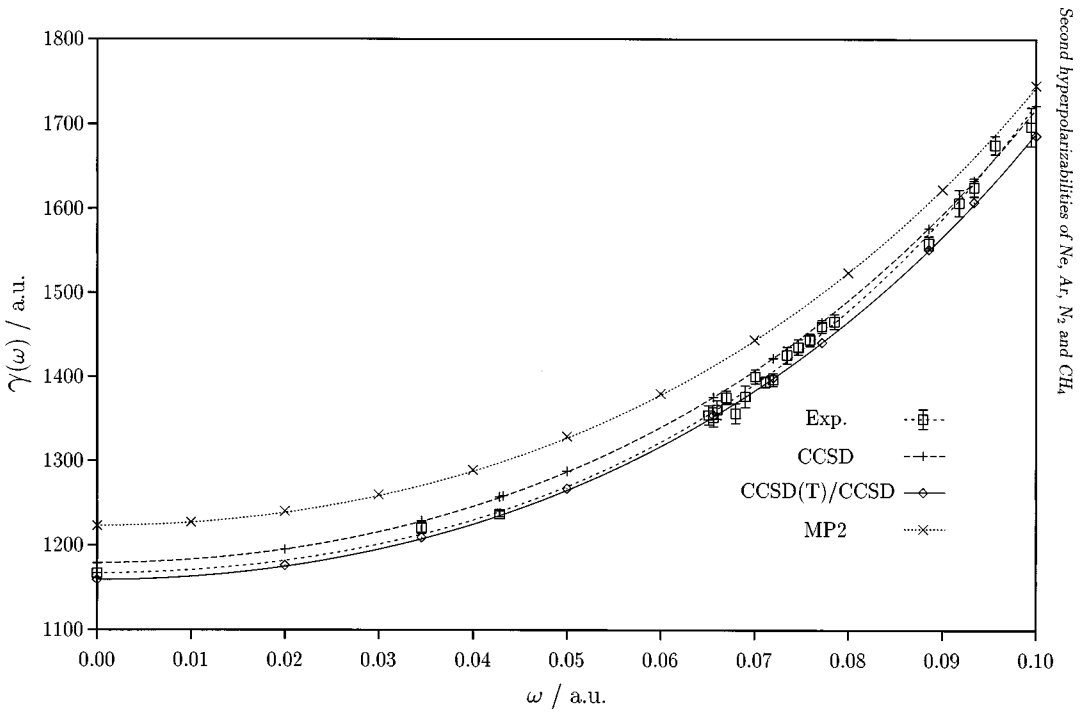


FIG. 4. Electric field induced second harmonic generation in argon. Comparison of the CCSD and the CCSD(T)/CCSD response curves with the experimental results (Refs. 1–3) and the CCSD(T)/MP2 dispersion curve of Rice (Refs. 5,9,48). The line through the experimental results is the fit of Ref. 3.

TABLE X. Comparison of the experimental data for dc Kerr effect, ESHG and THG for Ne with the CCSD response results multiplied by the factor $\gamma^{\mathrm{CCSD(T)}}_{\text{t-aug-cc-pVC5Z}}(0)/\gamma^{\mathrm{CCSD\ resp}}_{\text{t-aug-cc-pV5Z}}(0)$ to account approximately for core correlation and connected triples.

		$\gamma_K^{\mathrm{dc\ Kerr}}(\omega)$		$\gamma_{\|\|}^{\mathrm{ESHG}}(\omega)$		$\gamma_{\|\|}^{\mathrm{THG}}(\omega)$	
λ/nm	ω/a.u.	CCSD	Expt	CCSD	Expt	CCSD	Expt
1319.0	0.034544	107.8		109.2	111.0 ± 0.8[b]	111.4	
1064.0	0.042823	108.2		110.4	109.9 ± 0.5[b]	113.8	90 ± 45[d]
1055.0	0.043188	108.2		110.4		113.9	79.7 ± 8[e]
694.3	0.065625	109.6		115.0	126.4 ± 4.1[c]	123.8	108 ± 18[f]
632.8	0.072003	110.2	101 ± 8[a]	116.7		127.8	
514.5	0.088558	111.8		122.2	122.2 ± 0.4[b]	140.8	
488.0	0.093368	112.3		124.1	123.5 ± 0.5[b]	145.6	

[a]Reference 54.
[b]References 3,70,4.
[c]Reference 71.
[d]Reference 53.
[e]Reference 52.
[f]Reference 51.

an orbital relaxed CCSD(T) finite field calculation $\gamma_0^{\mathrm{Ar}} = 1159$ a.u. Accounting for these additional correlation effects by a multiplicative correction of the frequency-dependent CCSD results as for neon we obtained the result in Table XI. The respective dispersion curve in Fig. 4 has mean absolute and maximum deviations from the experimental points of 0.8% and −2.6%, respectively. For shorter wavelenghts the deviations become somewhat larger. The curvature of the calculated dispersion curve is slightly smaller than that for the fit through the experimental data. This is likely an effect of the missing contributions from connected triples and higher excitations to the dispersion of $\gamma_{||}(\omega)$. As for neon, the remaining uncertainity of the final estimates for γ_0^{Ar} due to basis set and correlation effects are estimated to be ≈ 1%–3%, although a smaller mean deviation from the experimental ESHG data are found.

Since CCSD response calculations for other optical proccesses do not face any additional problems, we expect that the CCSD dispersion curves for the dc Kerr effect, degenerate four wave mixing and third harmonic generation have about the same accuracy as the CCSD response calculations for $\gamma_{||}^{\mathrm{ESHG}}(\omega)$. The experimental situation however, is different: Only few measurements have been published for the dc Kerr effect and third harmonic generation in neon and argon and most of the experiments have uncertainities which are much larger than those of the ESHG experiments.

The THG hyperpolarizability of neon has been measured for three different wavelengths. From these three experiments only the first measurement by Ward and New[51] at λ = 694.3 nm is in fair agreement with the *ab initio* results. The value obtained by Lehmeier *et al.*[52] at 1055 nm is about 30% too small and the recent value of Li *et al.*[53] measured at

TABLE XI. Comparison of the experimental data for dc Kerr effect, ESHG and THG for Ar with the CCSD response results multiplied by the factor $\gamma^{\mathrm{CCSD(T)}}_{\text{t-aug-cc-pV5Z}}(0)/\gamma^{\mathrm{CCSD\ resp}}_{\text{t-aug-cc-pV5Z}}(0)$ to account approximately for core correlation and connected triples.

		$\gamma_K^{\mathrm{dc\ Kerr}}(\omega)$		$\gamma_{\|\|}^{\mathrm{ESHG}}(\omega)$		$\gamma_{\|\|}^{\mathrm{THG}}(\omega)$	
λ/nm	ω/a.u.	CCSD	Expt	CCSD	Expt[e]	CCSD	Expt
1319.0	0.034544	1175		1209	1220 ± 7	1261	
1064.0	0.042823	1185		1237	1236 ± 4	1321	1840 ± 920[f]
1055.0	0.043188	1185		1238		1324	1055 ± 105[g]
694.3	0.065625	1219		1354	1352 ± 11	1600	1525 ± 242[h]
632.8	0.072003	1232	1248 ± 10[b]	1399	1397 ± 8	1720	
590.0	0.077226	1244		1441	1460 ± 8	1849	
514.5	0.088558	1272	1211 ± 35[c]	1552	1559 ± 8	2191	
488.0	0.093368	1286		1608	1626 ± 7	2377	
457.9	0.099505	1304[a]	1187 ± 96[d]	1687[a]	1698 ± 23		

[a]Interpolated from a fit to the calculated points.
[b]Reference 6, for the same frequency in a previous experiment (Ref. 54) 1171 ± 80 a.u. was obtained.
[c]Reference 72.
[d]Reference 73.
[e]References 3,1. The experimental results are only listed for some representative frequencies. Compare also with Fig. 4 which includes all experimental results from Refs. 3,1.
[f]Reference 53.
[g]Reference 52.
[h]Reference 51.

TABLE XII. Bond length dependence of $\gamma_{||}$ for N_2, calculated at the CCSD level using the t-aug-cc-pVTZ basis.

r_{NN}/a.u.	γ_0	$\lambda=694.3$ nm				$\lambda=457.9$ nm			
		Kerr [a]	DFWM	ESHG	THG	Kerr [a]	DFWM	ESHG	THG
1.800	714.0	747.5	781.1	817.8	945.0	794.5	884.6	990.4	1458.9
1.900	772.6	809.2	846.2	886.6	1026.8	860.7	960.0	1076.8	1597.2
2.074	903.0	947.0	992.1	1041.1	1212.2	1009.2	1130.4	1273.4	1919.9
2.100	925.5					1034.9	1160.1	1307.8	1977.7
2.200	1019.1	1070.2	1122.8	1180.1	1380.8	1142.4	1284.5	1452.7	2224.6
2.300	1123.3					1262.7	1424.6	1617.0	2512.4
2.400	1237.0	1302.3	1370.2	1444.1	1705.5	1394.7	1579.4	1799.8	2842.2
$\langle 0\|\gamma\|0\rangle$	915.0	959.8	1005.7	1055.6	1229.8	1023.0	1146.5	1292.2	1952.4

[a]For the dc Kerr effect the table lists $\gamma_K(\omega)$.

1064 nm has a too large uncertainty to be useful in a comparison with the *ab initio* results. For argon the findings are similar: we obtain reasonable agreement with the experiment by Ward and New[51] at 694.3 nm, but significant disagreement with the newer measurement by Lehmeier *et al.*[52] for 1055 nm, and the recent experiment by Li *et al.*[53] for 1064 nm has too large an uncertainty to be useful.

For the dc Kerr effect in neon only one measurement by Buckingham and Dunmur[54] has been reported in the literature. Its value of 101 ± 8 a.u. measued for $\lambda=632.8$ nm falls with its error bar below the CCSD response results (cmp. Table X). From the four dc Kerr measurements for argon, we obtain only good agreement with the most recent experiment by Shelton and Palubinskas[6] at 632.8 nm. The earlier experiment by Buckingham and Dunmur[54] for the same wavelength is also in agreement with the CCSD calculations, but has a large uncertainity. The experimental results for 514.4 and 457.9 nm fall both with their error bars below the CCSD dispersion curve.

B. Nitrogen

The analysis of the calculations for Ne and Ar showed that by the combination of CCSD response calculations with large correlation consistent basis sets and estimates for connected triples and core correlation we can for both atoms obtain agreement with the ESHG experiments within a few percent. To reach a similar accuracy for molecules is much more demanding. For a direct comparison with the experimental data, one must in addition account for vibrational averaging and for the pure vibrational and rotational contributions to the hyperpolarizabilities.

For the diatomic example N_2, the pure vibrational and rotational contributions to the ESHG processes were estimated by Shelton.[3] From his work a fit through the experimental ESHG data are available which was corrected for these contributions and can be compared directly with vibrational averaged electronic hyperpolarizabilities from *ab initio* calculations. Vibrational averaging has for N_2 only a small effect of $\approx 1\%$ on γ_0 which increases slowly with the frequency. We therefore performed vibrational averaging only for the static limit and for two wavelengths: 694.3 and 457.9 nm. We used for these calculations a CCSD(T) potential energy curve obtained with the same basis set and the CCSD hyperpolarizability results listed in Table XII. For the remaining frequencies we interpolated the zero point vibrational correction using the expression[55] $\Delta\gamma_{||}^{\mathrm{ZPVA}}(\omega_0;\omega_1,\omega_2,\omega_3)\approx\Delta\gamma_0^{\mathrm{ZPVA}}(1+a\omega_L^2+b\omega_L^4)$ with $\omega_L^2=\omega_0^2+\omega_1^2+\omega_2^2+\omega_3^2$. The parameters a and b were determined by a least square fit to the results in Table XII. The vibrational averaged CCSD response results for the dc Kerr effect, DFWM, ESHG and THG are given in Table XIII. The electric field induced second harmonic generation (ESHG) results are again of particular interest. In the static limit and for small frequencies the vibrational averaged CCSD response results are in almost perfect agreement with the fit through the experimental ESHG data for the electronic contribution (see Tables VIII and XIV and Fig. 5). However, from the basis set study in Sec. IV we know that for the t-aug-cc-pVTZ basis set, which we used for the frequency-dependent calculations, the remaining basis set error is not negligible, since the extrapolated ''best estimate'' for the unrelaxed CCSD basis set limit is about 36 a.u. smaller than the t-aug-cc-pVTZ result. Combining the extrapolated unrelaxed CCSD value of 867 a.u. with the effect of connected triples from Table III and including the zero point vibrational correction from the CCSD calculation (12 a.u., cmp. Table XII), we arrive at a result of $\gamma_0^{e,\mathrm{N_2}}=894$ a.u. for the static hyperpolarizability of N_2. This has to be compared with the estimate obtained by Shelton from the experimental ESHG

TABLE XIII. Dispersion curves for different optical processes for N_2, calculated at the CCSD level using the t-aug-cc-pVTZ basis. Listed are the vibrational averages of $\gamma_{||}$ for DFWM, ESHG and THG and of γ_K for the Kerr effect.

λ/nm	ω/a.u.	Kerr	DFWM	ESHG	THG
1055.0	0.043188	933.9	952.5	972.1	1034.6
694.3	0.065625	959.7	1005.5	1055.4	1230.0
632.8	0.072003	969.2	1025.7	1088.0	1313.8
590.0	0.077226	977.8	1044.2	1118.3	1395.5
514.5	0.088558	998.9	1091.1	1196.7	1626.6
488.0	0.093368	1008.9	1114.0	1236.0	1754.2
457.9	0.099505	1022.8	1146.4	1292.4	1952.3

TABLE XIV. Comparison of the experimental data for the dc Kerr effect, ESHG and THG for N_2 with the vibrational averaged CCSD response results multiplied by the factor $\gamma^{\mathrm{CCSD(T)}}_{\text{best estimate}}(0)/\gamma^{\text{CCSD resp}}_{\text{t-aug-cc-pVTZ}}(0)$ to account approximately for connected triples and remaining basis set effects (see text for details).

		$\gamma_K^{\text{dc Kerr}}(\omega)$		$\gamma_{\|\|}^{\text{ESHG}}(\omega)$		$\gamma_{\|\|}^{\text{THG}}(\omega)$	
λ/nm	ω/a.u.	CCSD	Exp.	CCSD	Expt [a]	CCSD	Expt
1055.0	0.043188	912.5		949.8		1010.8	954±95[c]
694.3	0.065625	937.6		1031.2	1057.6±6.4	1201.3	1295±206[d]
632.8	0.072003	947.0	1443±160[b]	1063.1	1095.6±4.6	1283.6	
590.0	0.077226	955.4		1092.7	1132.0±4.2	1363.4	
514.5	0.088558	975.9		1169.2	1208.7±6.2	1589.2	
488.0	0.093368	985.8		1207.7	1253.3±6.3	1714.0	
457.9	0.099505	999.4		1262.8	1327.5±14..3	1907.5	

[a]References 1,2.
[b]Reference 58.
[c]Reference 52.
[d]Reference 51.

data by extrapolation: $\gamma_{||}^{e,\mathrm{N_2}}(0)=917\pm9$ a.u. The deviation between the two estimates is small, only 2.5%, and probably partly due to remaining basis set effects and higher-order correlation contributions.

Notwithstanding this remaining uncertainity, the comparison of the dispersion curve from the vibrational averaged calculations with the experimental ESHG data demonstrate that the CCSD response approach gives an accurate description of the dispersion contribution. First for $\lambda<570$ nm the CCSD dispersion curve falls somewhat below Shelton's fit, because its curvature is slightly smaller. Again, we attribute this to the contributions from connected triples which are not included in the frequency-dependent calculations. Connected triples tend to lower excitation energies and therefore it is expected that they increase the dispersion of dynamic properties. We thus obtain also for the diatomic example, N_2, a good agreement with the ESHG experiments, although the remaining deviation is considerably larger as for Ne and Ar.

The third harmonic generation hyperpolarizability of N_2 has been measured by Ward and New[51] for 694.3 nm and

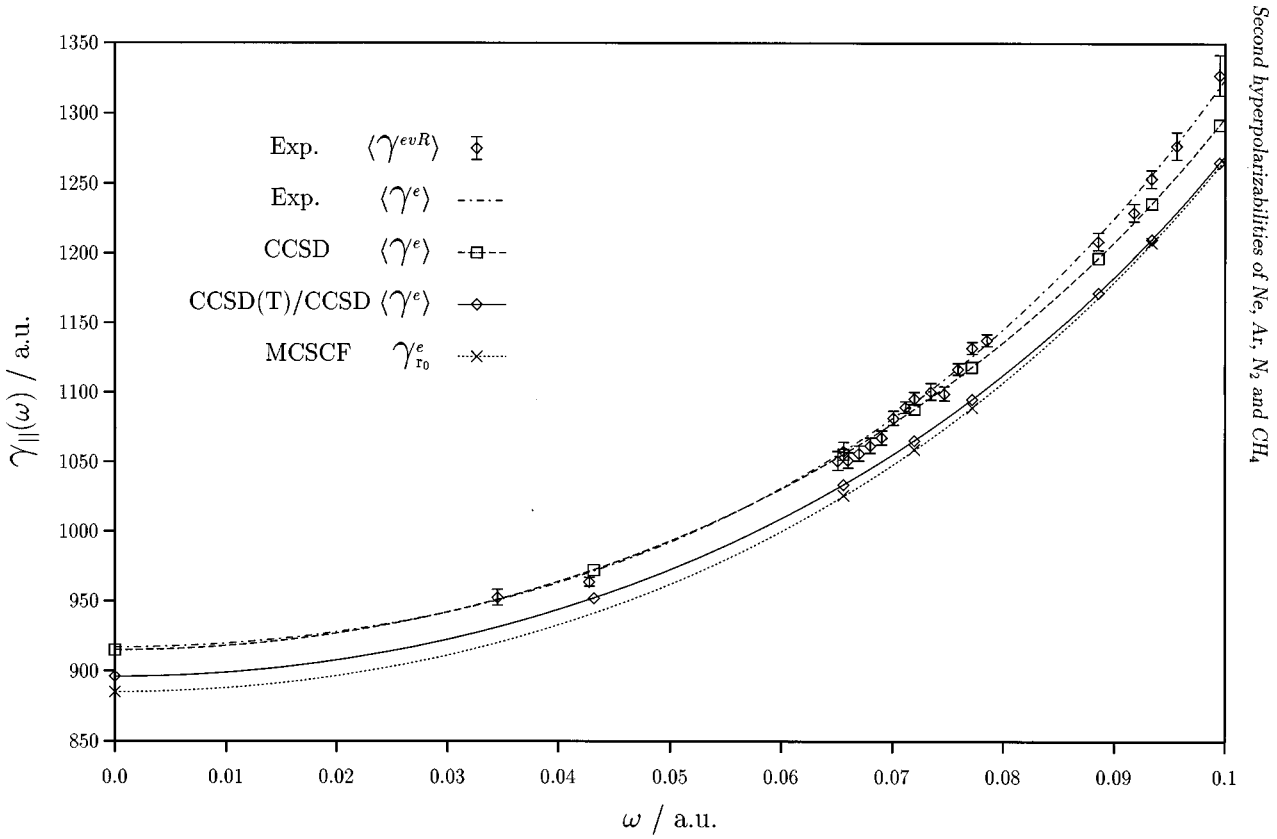


FIG. 5. Electric field induced second harmonic generation in nitrogen (N_2). Comparison of the vibrational averaged CCSD and the extrapolated CCSD(T)/CCSD dispersion curves with the experimental results (Refs. 1–3) and the MCSCF dispersion curve of Luo *et al.* (Ref. 65). The line through the measured points is the fit of Ref. 3 to the ESHG data after subtraction of the pure vibrational and rotational contributions.

TABLE XV. Dispersion curves for different optical processes for CH_4, calculated at the CCSD level using the t-aug-cc-pVTZ basis, $r_{CH}=2.052$ a.u.

λ/nm	ω/a.u.	Kerr [a]	DFWM	ESHG	THG
1319.0	0.034544	2407.3	2450.3	2494.7	2635.2
1064.0	0.042823	2430.6	2498.2	2568.8	2799.2
671.5	0.067853	2535.1	2722.1	2929.5	3716.0
590.0	0.077357	2589.6	2845.2	3137.6	4350.7
514.5	0.088559	2665.6	3024.8	3454.4	5507.8
476.5	0.095621	2720.7	3161.1	3705.2	6635.7

[a]For the dc Kerr effect the table lists γ_K. For the definition of γ_K see Sec. III.

Lehmeier *et al.*[52] for 1055 nm. In the former experiment the ratio $\gamma^{THG}_{N_2}/\gamma^{THG}_{He}$ was determined at 694.3 nm as 26.75 ± 4.25. Using the accurate *ab initio* results for γ^{THG}_{He} from Bishop and Pipin[7] one obtains $\gamma^{THG}_{N_2}(\lambda=694.3\ \text{nm})=1295 \pm 206$ a.u. Taking into account the large uncertainity of the experimental result, this is in fair agreement with the CCSD response result, which is 1201 a.u. (see Table XIV). The rovibrational contribution to $\gamma^{THG}_{N_2}(\lambda=694.3\ \text{nm})$ was estimated by Shelton[56,57] as -0.64 a.u. and is thus insignificant for this comparison. Lehmeier *et al.* obtained for $\lambda=1055$ nm a ratio of $\gamma^{THG}_{N_2}/\gamma^{THG}_{He}=21.1\pm2.1$, corresponding to $\gamma^{THG}_{N_2}=954\pm95$ a.u., which is somewhat smaller than the CCSD response result of $\gamma^{THG}_{N_2}=1010.8$ a.u., although the *ab initio* result is within the uncertainity of the experiment.

The only experimental result for the dc Kerr hyperpolarizability of N_2 is from Ref. 58 and was measured at 632.8 nm as 1443 ± 160 a.u., which is much larger than the *ab initio* result of 949.1 a.u. for the electronic contribution. The vibrational contribution to $\gamma_K(632.8\ \text{nm})$ was estimated in Refs. 56,57 as 0.5 a.u. and is thus negligible, but the rotational contribution was estimated[5] as large as 4670 a.u. and thus hinders a meaningful comparison.

C. Methane

The methane molecule has 9 vibrational degrees of freedom and vibrational averaging using numerical integration is therefore prohibitive. For polyatomic molecules the zero point vibrational correction and the pure vibrational contribution can only be otained using perturbation theory. This requires the evaluation of derivatives with respect to the normal coordinates for the dipole moment, the frequency-dependent polarizability and the first and second hyperpolarizability. Because the determination of these derivatives was out of the scope of the present investigation, we have determined only the electronic hyperpolarizabilities at the equilibrium geometry and have taken the values for the zero point vibrational correction and for the pure vibrational contribution from the literature. The rotational contribution to the hyperpolarizability vanishes for spherical-top molecules like CH_4.

In Table XV the CCSD response results for the four optical processes obtained with the t-aug-cc-pVTZ basis are listed. A graphical presentation of the results is given in Fig. 2. The zero point vibrational correction for $\gamma^{ESHG}_{CH_4}$ has recently been calculated by Bishop and Sauer[59] using the MCSCF response theory combined with a numerical differencing technique for the derivatives of γ with respect to the normal coordinates. To correct the CCSD dispersion curve for $\gamma^{ESHG}_{||}(\omega)$ we have fitted the MCRPA results of Ref. 59 to the expression $\Delta\gamma^{ZPVA}_{||}(\omega_L^2)=\Delta\gamma^{ZPVA}_0(1+a\omega_L^2+b\omega_L^4+c\omega_L^6)$. The pure vibrational contribution to $\gamma^{ESHG}_{CH_4}$ has been determined by Bishop and Pipin[60] based on the perturbational approximation introduced by Bishop and Kirtmann[61] using Hartree-Fock values for the necessary derivatives of the dipole moment, the polarizability and the first hyperpolarizability. Adding the pure vibrational contributions of Ref. 60 and the ZPVA correction to the results of the CCSD response calculation we obtained the ESHG hyperpolarizabilities in Table XVI. The dispersion curves for $\gamma^{ESHG}_{||}(\omega)$ in methane are shown in Fig. 6 in comparison with the experimental results and the MCSCF calculations of Ref. 59. In contrast to N_2, the zero point vibrational averaging and the vibrational contribution for methane are not small corrections: depending on the frequency, they account for ≈10%–20% of the total hyperpolarizability. But even though these effects are treated more approximately, we obtain a very good agreement with the experimental ESHG results with mean absolute and maximum deviations of respectively 1.5% and 4.4%, where the largest deviation is found at 1319 nm. Also the static limit of the electronic hyperpolarizability is in good agreement with the estimates extrapolated from the experimental ESHG data: the CCSD response result in the t-aug-cc-pVTZ basis plus $\Delta\gamma^{ZPVA}$ from Ref. 59 leads to $\gamma^{e,CH_4}_{||}(0)=2650$ a.u., which has to be compared with the estimates derived from the experimental results by Shelton[3] without further modifications of the measured data, 2590 a.u., and by Bishop and Pipin[60] after correction for the pure vibrational contribution, 2607 a.u.

To obtain more information on the remaining uncertainity of the electronic contribution, we performed a CCSD(T) finite field calculation in the d-aug-cc-pVTZ basis which led to $\gamma^{CH_4}_{||}(0)=2294$ a.u. The unrelaxed CCSD value in the same basis is 2364 a.u. Thus, the sum of orbital relaxation effect and the contribution of connected triples is only small: -70 a.u. or -3%. Combining the best estimate of the CCSD basis set limit obtained in Sec. IV with $\Delta\gamma^{ZPVA}$ and the orbital relaxation and triples effect, we get a best estimate for the static electronic second hyperpolarizability of $\gamma^{e,CH_4}_{||}(0)=2533$ a.u. The uncertainity of the CCSD result due to basis set incompleteness was estimated in Sec. IV to be $\approx\pm35$ a.u. The additional uncertainity introduced by the higher-order correlation effects which we have not included and by the approximations used in Ref. 60 for the calculation of $\Delta\gamma^{ZPVA}$ are likely of a similar magnitude. Thus the total uncertainity of $\gamma^{e,CH_4}_{||}(0)$ is estimated to be about ±70 a.u. or $\pm3\%$. Little is known about the uncertainity of the pure vibrational contribution taken from Refs. 59,60. Therefore it is difficult to assess the uncertainity of the frequency-dependent results.

Shelton and Palubinskas[6] have recently measured the dc Kerr hyperpolarizability for methane for seven different frequencies. To compare the CCSD dispersion for the dc Kerr

TABLE XVI. Comparison of the experimental data for dc Kerr effect, ESHG and THG in CH_4 with the *ab initio* calculated results which iclude zero point vibrational correction and the pure vibrational contribution.

		$\gamma_K^{\text{dc Kerr}}(\omega)$		$\gamma_{\|\|}^{\text{ESHG}}(\omega)$		$\gamma_{\|\|}^{\text{THG}}(\omega)$	
λ/nm	ω/a.u.	CCSD	Expt. [b]	CCSD	Expt. [e]	CCSD [f]	Expt. [g]
1319.0	0.034544	2894		2717	2603±11	2974	
1092.0	0.041725	2920 [a]	2855±21				
1064.0	0.042823	2925		2822	2833±10	3173	
763.5	0.059677	3004 [a]	2967±16				
694.3	0.065625	3039 [a]				4162 [a]	3997±120
671.5	0.067853	3054		3312	3311±10	4308	
632.8	0.072003	3081 [a]	3070±11[c]				
589.0	0.077357	3120	3132±27	3575	3613±9	5112	
514.5	0.088559	3212	3236±19	3975	4060±23	6581	
488.0	0.093368	3256 [a]	3286±24				
476.5	0.095621	3278		4291	4414±24	7997	
457.9	0.099505	3317 [a]	3360±14[d]				

[a]Interpolated between the calculated points.
[b]Reference 6.
[c]In a previous experiment (Ref. 74) at the same wavelength a value of 2887±144 a.u. was obtained.
[d]In a previous experiment (Ref. 73) at the same wavelength a value of 3063±160 a.u. was obtained.
[e]References 3,75.
[f]Only electronic contribution, see text for explanation.
[g]Reference 62.

effect with the experimental results, we estimated the zero point vibrational correction from the MCRPA results for ESHG from Ref. 59, assuming that $\Delta\gamma^{\text{ZPVA}}(\omega_L^2)$ for the dc Kerr effect and ESHG follows the same dispersion curve in the effective frequency ω_L^2. We thereby neglect the small difference between γ_K and $\gamma_{||}$ and the fact that $\Delta\gamma^{\text{ZPVA}}(\omega_L^2)$ for the dc Kerr effect and ESHG differ in sixth order in ω_L. The pure vibrational contribution is again taken from Ref.

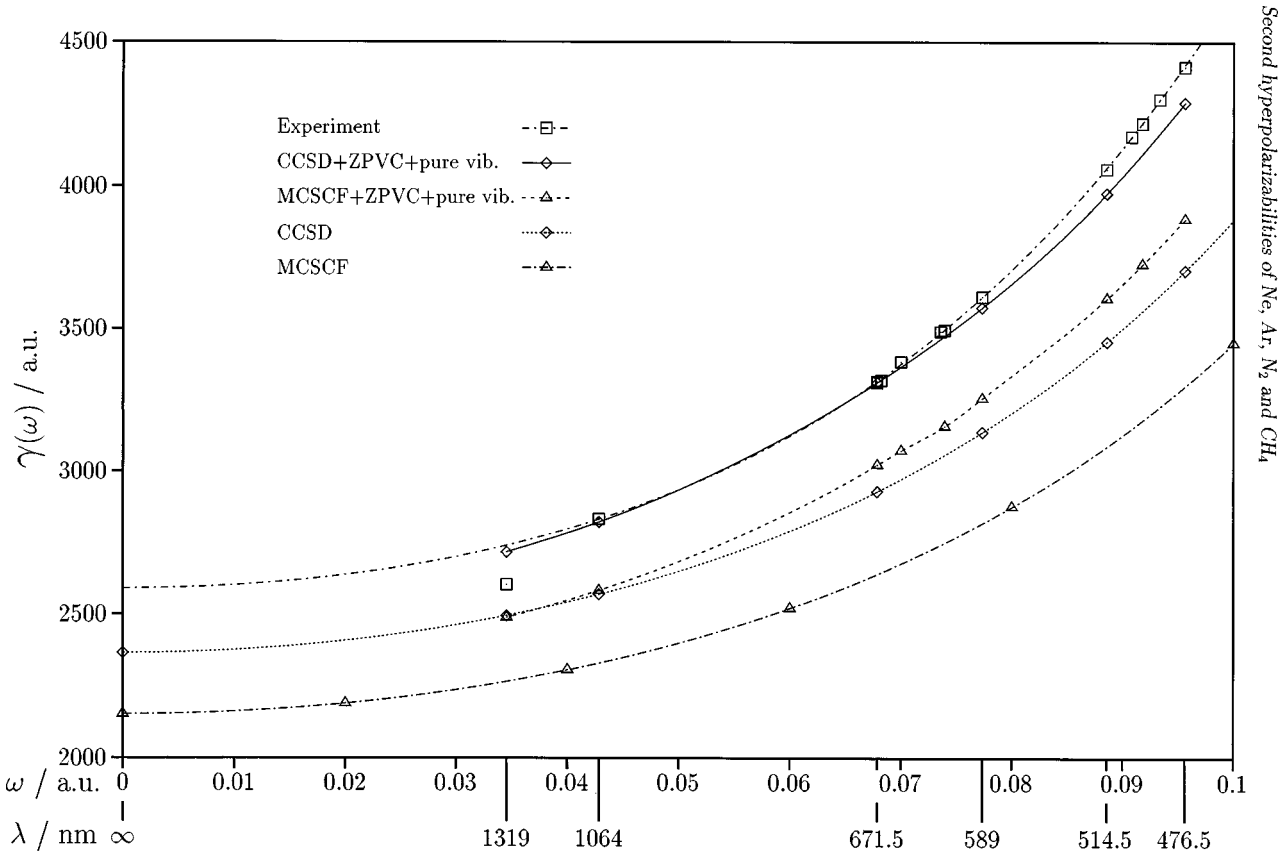


FIG. 6. Electric field induced second harmonic generation in methane (CH_4). Comparison of the experimental results of Refs. 1–3 with the CCSD response results at the equilibrium distance $\gamma_{r_0}^e$, and with the zero point vibrational corrections $\Delta\gamma^{\text{ZPVA}}$ and the pure vibrational contribution γ^v from Refs. 59,60 added (see text for details).

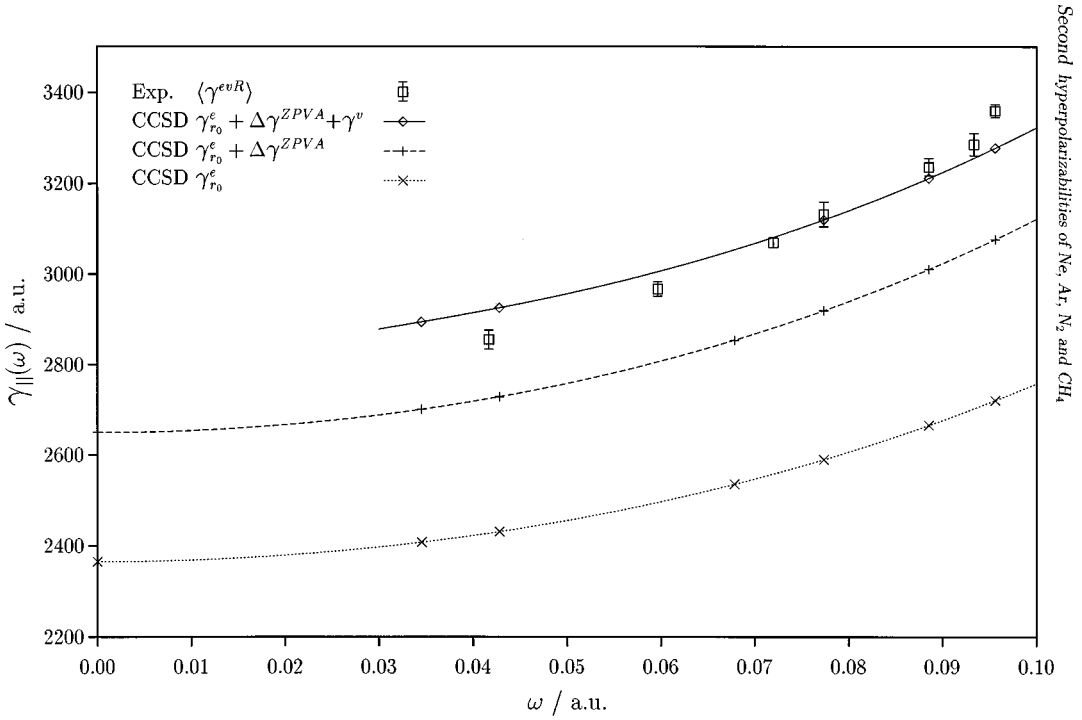


FIG. 7. dc Kerr effect in methane (CH_4). Comparison of the experimental results of Ref. 6 with the CCSD response results at the equilibrium distance $\gamma^e_{r_0}$, and with the zero point vibrational corrections $\Delta\gamma^{\mathrm{ZPVA}}$ and the pure vibrational contribution γ^v from Refs. 59,60 added (see text for details).

60. The results obtained by adding these contributions to the CCSD response values are compared with the experimental results from Shelton and Palubinskas in Fig. 7. On the average we obtain a good agreement between the calculated curve and the experimental results of Ref. 6 with deviations of only 0.5%–2.5%. But the dispersion of the *ab initio* curve is distinctly too small to fit to the experimental points: for the lower frequencies the calculated results are too large by $\approx$2.5%, while for the higher frequencies they are too small by $\approx$2.5%. Although it is expected that the inclusion of connected triples in the response calculations would slightly increase the dispersion of the electronic contribution, this deviation can hardly be traced back to this effect, since the comparison of the ESHG data showed that the dispersion of the electronic hyperpolarizabilities is well described at the CCSD response level. It was already observed by Shelton and Palubinskas[6] that the calculated values for the vibrational hyperpolarizability of Ref. 60 disagreed in size and dispersion with the analysis of the experimental results. Is is therefore likely that a large fraction of the discrepancy between the *ab initio* dispersion curve and the Kerr measurements is a consequence of the approximations used in Ref. 60 for the calculation of the vibrational contribution. Nevertheless, this is the first time that for a dc Kerr hyperpolarizability agreement within a few percent is obtained between *ab initio* calculations and experimental measurements.

For the third harmonic generation hyperpolarizability of CH_4 only one measurement is reported in the literature. Ward and Elliot[62] have determined the ratio of $\gamma^{\mathrm{THG}}_{\mathrm{CH_4}}/\gamma^{\mathrm{THG}}_{\mathrm{He}}$ at 694.3 nm as 82.5 ± 2.5 corresponding to an absolute value for $\gamma^{\mathrm{THG}}_{\mathrm{CH_4}}$ of 3997 ± 120 a.u. Because the vibrational contribution and the zero point vibrational correction are not known for $\gamma^{\mathrm{THG}}_{\mathrm{CH_4}}$, an accurate comparison with the CCSD response results is not possible. From an interpolation of the numbers in Table XV we obtain $\gamma^{\mathrm{THG}}_{r_0}(694.3\ \mathrm{nm})=3600$ a.u. The vibrational hyperpolarizability is for THG at optical frequencies far above vibrational resonances usually smaller than for ESHG and should be almost negligible here. Extrapolating $\Delta\gamma^{\mathrm{ZPVA}}$ from the MCRPA data of Ref. 59 in the same way as for the dc Kerr effect, we obtain for the electronic contribution the rough estimate of 4162 a.u., which indicates a reasonable agreement between the *ab initio* calculation and the experimental measurement.

VII. CONCLUDING REMARKS

We have presented a coupled cluster response study of the frequency-dependent second hyperpolarizability of four example systems: Ne, Ar, N_2 and CH_4. Basis set studies were performed at the SCF and the unrelaxed CCSD level using sequences of correlation consistent basis sets. The largest basis sets employed for N_2 and CH_4 included 326 and 353 basis functions, respectively. The hierarchical structure of the correlation consistent basis sets was employed to get results close to the basis set limit and to estimate the remaining error. We found that in correlated calculations, once a certain augmentation level is reached, the second hyperpolarizability results tend to decrease if the description of the valence part is improved in the series TZ - QZ - 5Z. Considering only saturation of the basis with respect to augmentation with diffuse functions, as was often done in the literature, gives for the examples studied here significantly too large results and leads to too small estimates for the remaining basis set errors.

A comparison of the orbital-unrelaxed CCS, CC2 and CCSD response approaches with SCF and orbital-relaxed CCSD and CCSD(T) calculations shows, that, at least for the systems studied here, the unrelaxed coupled cluster response hierarchy provides static isotropic hyperpolarizabilities γ_0 of a similar or even better accuracy than relaxed coupled cluster calculations at the same level. For the four examples studied here, we found that the difference between unrelaxed CCSD and relaxed CCSD(T) results is distinctly smaller than the difference between relaxed CCSD and CCSD(T). We also compared the performance of SCF (RPA) and CCS, CC2 and CCSD for the dispersion of the third harmonic generation in Ne, Ar, N_2 and CH_4. We found that, contrary to presumptions in the literature, the dispersion of hyperpolarizabilities is as sensitive to the correlation treatment as the static limit result. In the coupled cluster response hierarchy CCS, CC2, CCSD we obtain a systematic improvement of the dispersion at each level and for the CCSD response approach the agreement with experiment is for all four examples very good.

A detailed comparison with the available experimental data for neon and argon demonstrates that by carrying out sequences of CCSD response calculations with series of correlation consistent basis sets we can reach a level of accuracy for frequency-dependent hyperpolarizabilities of many-electron systems which has not been accessible in previous *ab initio* calculations. Accounting for connected triples and core correlation, we obtained for neon and argon agreement with the most accurate ESHG experiments within $\approx$1%.

For molecules it is much more difficult to advance the treatment to a point where similar good agreement with experiment can be expected. To obtain results which can be compared directly with the experimental data, we must take into account the effect of vibrational averaging and the pure vibrational contributions. We have taken these contributions from the literature and combined them with the results of the coupled cluster calculations. On doing so, we have obtained ESHG hyperpolarizabilities for N_2 and CH_4 which agree within $\approx$2% with the experimental results.

Similar good agreement is obtained with the newest measurements for the dc Kerr hyperpolarizability of Ar and CH_4, where the calculated results agree with the experimental values within 1.5% and 3%, respectively. The agreement is less favorable with older dc Kerr measurements and for third harmonic generation, because the uncertainities of the experimental data are larger and because the estimates for the rotational and vibrational contributions are more approximate. For the third harmonic generation the uncertainities of the experimental results are too large to allow for a comparison within a couple of percent. We expect the CCSD response results for the THG to be more reliable than the available experimental data.

ACKNOWLEDGMENTS

One of the authors (C.H.) thanks the European Commission for financial support through the Training and Mobility of Researchers (TMR) Program (ERBFMBICT 96.1066). This work has been supported by the Danish Natural Research Council (Grant No. 9600856).

[1] Y. Mizrahi and D. P. Shelton, Phys. Rev. Lett. **55**, 696 (1985).
[2] Y. Mizrahi and D. P. Shelton, Phys. Rev. A **31**, 3145 (1985).
[3] D. P. Shelton, Phys. Rev. A **42**, 2578 (1990).
[4] D. P. Shelton and E. A. Donley, Chem. Phys. Lett. **195**, 591 (1992).
[5] D. P. Shelton and J. E. Rice, Chem. Rev. **94**, 3 (1994).
[6] D. P. Shelton and J. J. Palubinskas, J. Chem. Phys. **104**, 2482 (1996).
[7] D. M. Bishop and J. Pipin, J. Chem. Phys. **91**, 3549 (1989).
[8] P. R. Taylor, T. J. Lee, J. E. Rice, and J. Almlöf, Chem. Phys. Lett. **163**, 359 (1989).
[9] J. E. Rice, P. R. Taylor, T. J. Lee, and J. Almlöf, J. Chem. Phys. **94**, 4972 (1991).
[10] J. E. Rice, G. E. Scuseria, T. Lee, P. R. Taylor, and J. Almlöf, Chem. Phys. Lett. **191**, 23 (1992).
[11] O. Christiansen and P. Jørgensen, Chem. Phys. Lett. **207**, 367 (1993).
[12] D. P. Shelton and R. E. Cameron, Rev. Sci. Instrum. **59**, 430 (1988).
[13] D. P. Shelton, Rev. Sci. Instrum. **64**, 917 (1993).
[14] H. Hettema, H. J. A. Jensen, P. Jørgensen, and J. Olsen, J. Chem. Phys. **97**, 1174 (1992).
[15] D. Jonsson, P. Norman, and H. Ågren, J. Chem. Phys. **105**, 6401 (1996).
[16] C. Hättig, O. Christiansen, and P. Jørgensen, Chem. Phys. Lett. **269**, 428 (1997).
[17] C. Hättig, O. Christiansen, and P. Jørgensen, Chem. Phys. Lett. **282**, 139 (1998).
[18] D. M. Bishop, J. Pipin, and S. M. Cybulski, Phys. Rev. A **43**, 4845 (1991).
[19] J. Olsen and P. Jørgensen, J. Chem. Phys. **82**, 3235 (1985).
[20] J. Olsen and P. Jørgensen, *Time-Dependent Response Theory with Applications to Self-Consistent Field and Multiconfigurational Self-Consistent Field Wave Functions*, in *Modern Electronic Structure Theory*, edited by D. R. Yarkony (World Scientific, Singapore, 1995), Vol. 2, Chap. 13, pp. 857–990.
[21] H. Koch and P. Jørgensen, J. Chem. Phys. **93**, 3333 (1990).
[22] O. Christiansen, P. Jørgensen and C. Hättig, Int. J. Quantum Chem. **68**, 1 (1998).
[23] C. Hättig and B. A. Hess, Chem. Phys. Lett. **233**, 359 (1995).
[24] O. Christiansen, H. Koch, and P. Jørgensen, J. Chem. Phys. **103**, 7429 (1995).
[25] O. Christiansen, H. Koch, A. Halkier, P. Jørgensen, T. Helgaker, and A. M. Sanchez de Meras, J. Chem. Phys. **105**, 6921 (1996).
[26] O. Christiansen, H. Koch, and P. Jørgensen, Chem. Phys. Lett. **243**, 409 (1995).
[27] H. Koch, O. Christiansen, P. Jørgensen, and J. Olsen, Chem. Phys. Lett. **244**, 75 (1995).
[28] O. Christiansen, H. Koch, P. Jørgensen, and J. Olsen Chem. Phys. Lett. **256**, 185 (1996).
[29] D. E. Woon and T. H. Dunning, J. Chem. Phys. **100**, 2975 (1994).
[30] P. W. Langhoff, S. T. Epstein, and M. Karplus, Rev. Mod. Phys. **44**, 602 (1972).
[31] T. Helgaker and P. Jørgensen, Theor. Chim. Acta **75**, 111 (1989).
[32] P. Jørgensen and T. Helgaker, J. Chem. Phys. **89**, 1560 (1988).
[33] D. M. Bishop, J. Chem. Phys. **100**, 6535 (1994).
[34] I. J. Bigio and J. F. Ward, Phys. Rev. A **9**, 35 (1974).
[35] K. P. Huber and G. Herzberg. *Molecular Spectra and Molecular Structure. IV. Constants of Diatomic Molecules* (Van Nostrand, New York, 1979).
[36] D. L. Gray and A. G. Robiette, Mol. Phys. **37**, 1901 (1979).
[37] P. Norman, D. Jonsson, O. Vahtras, and H. Ågren, Chem. Phys. **203**, 23 (1996).
[38] T. Helgaker, H. J. A. Jensen, P. Jørgensen, J. Olsen, K. Ruud, H. Ågren, T. Andersen, K. L. Bak, V. Bakken, O. Christiansen, P. Dahle, E. K. Dalskov, T. Enevoldsen, B. Fernandez, H. Heiberg, H. Hettema, D. Jonsson, S. Kirpekar, R. Kobayashi, H. Koch, K. V. Mikkelsen, P. Norman, M. J. Packer, T. Saue, P. R. Taylor, and O. Vahtras, DALTON, an electronic structure program, release 1.0, 1997.
[39] T. H. Dunning, J. Chem. Phys. **90**, 1007 (1989).
[40] R. A. Kendall, T. H. Dunning, and R. J. Harrison, J. Chem. Phys. **96**, 6796 (1992).
[41] D. E. Woon and T. H. Dunning, J. Chem. Phys. **98**, 1358 (1993).
[42] D. E. Woon and T. H. Dunning, J. Chem. Phys. **103**, 4572 (1995). The basis sets were obtained from the Extensible Computational Chemistry Environment Basis Set Database, Version 1.0, as developed and distributed by the Molecular Science Computing Facility, Environmental and Molecular Sciences Laboratory which is part of the Pacific Northwest Laboratory, P.O. Box 999, Richland, Washington 99352, USA, and funded by the U.S. Department of Energy. PNL is a multiprogram labo-

ratory operated by Batelle Memorial Institute for the U.S. Department of Energy under Contract No. DE-AC06-76RLO 1830.
[43] Since in coupled cluster response calculations nonrelaxed SCF orbitals are used, a frozen core approximation means for the CC response hierarchy that the frozen orbitals are also not polarized by the external field.
[44] E. A. Salter, H. Sekino, and R. J. Bartlett, J. Chem. Phys. **87**, 502 (1987).
[45] R. Kobayashi, H. Koch, P. Jørgensen, and T. J. Lee, Chem. Phys. Lett. **211**, 94 (1993).
[46] J. E. Rice and N. C. Handy, Int. J. Quantum Chem. **43**, 91 (1992).
[47] D. M. Bishop, Adv. Quantum Chem. **25**, 2 (1994).
[48] J. E. Rice, J. Chem. Phys. **96**, 7580 (1992).
[49] H. J. A. Jensen, P. Jørgensen, H. Hettema, and J. Olsen, Chem. Phys. Lett. **187**, 387 (1991).
[50] C. Hättig and P. Jørgensen, Chem. Phys. Lett. **283**, 109 (1998).
[51] J. F. Ward and G. H. C. New, Phys. Rev. **185**, 57 (1969).
[52] H. J. Lehmeier, W. Leupacher, and A. Penzkofer, Opt. Commun. **56**, 67 (1985).
[53] X. F. Li, A. L'Huillier, M. Ferray, L. A. Lompré, and G. Mainfray, Phys. Rev. A **39**, 5731 (1989).
[54] A. D. Buckingham and D. A. Dunmur, Trans. Faraday Soc. **64**, 1776 (1968).
[55] This power series is only well founded for $\Delta\gamma_{||}^{\mathrm{ZPVA}}$, but not for $\Delta\gamma_{K}^{\mathrm{ZPVA}}$. We use it here nevertheless also for the Kerr hyperpolarizability, since the difference between $\gamma_{||}$ and γ_K is for N_2 in the considered frequency range small and we expand here only a small correction.
[56] D. P. Shelton, Mol. Phys. **60**, 65 (1987).
[57] D. P. Shelton, Phys. Rev. A **36**, 3461 (1987).
[58] A. D. Buckingham, M. P. Bogaard, D. A. Dunmur, C. Hobbs, and B. J. Orr, Trans. Faraday Soc. **66**, 1548 (1970).
[59] D. M. Bishop and S. P. A. Sauer, J. Chem. Phys. **108**, 8502 (1997).
[60] D. M. Bishop and J. Pipin, J. Chem. Phys. **103**, 4980 (1995).
[61] D. M. Bishop and B. Kirtman, J. Chem. Phys. **95**, 2646 (1991).
[62] J. F. Ward and D. S. Elliot, J. Chem. Phys. **80**, 1003 (1984).
[63] J. Stiehler and J. Hinze, J. Phys. B **28**, 4055 (1995).
[64] M. Jaszuński, P. Jørgensen, and A. Rizzo, Theor. Chim. Acta **90**, 291 (1995).
[65] Y. Luo, O. Vahtras, H. Ågren, and P. Jørgensen, Chem. Phys. Lett. **205**, 555 (1993).
[66] H. Sekino and R. J. Bartlett, J. Chem. Phys. **98**, 3022 (1993).
[67] G. Maroulis, Chem. Phys. Lett. **226**, 420 (1994).
[68] H. Müller, J. Noga, and W. Kutzelnigg (unpublished).
[69] E. F. Archibong and A. J. Thakkar, J. Chem. Phys. **100**, 7471 (1994).
[70] D. P. Shelton, Phys. Rev. Lett. **62**, 2660 (1989).
[71] R. S. Finn and J. F. Ward, Phys. Rev. Lett. **26**, 285 (1971).
[72] S. Carusotto, E. Iacopini, and E. Polacco, Nuovo Cimento D **5**, 328 (1985).
[73] D. A. Dunmur, D. C. Hunt, and N. E. Jessup, Mol. Phys. **37**, 713 (1979).
[74] A. D. Buckingham and B. J. Orr, Trans. Faraday Soc. **65**, 673 (1969).
[75] D. P. Shelton, Phys. Rev. A **34**, 304 (1986).